



Models of Drought Hazard, Exposure, Vulnerability and Risk for Latin America

TECHNICAL REPORT

Hugo Carrão and Paulo Barbosa

European Commission – Joint Research Centre (EC-JRC)
Institute for Environment and Sustainability (IES)

October 27, 2015

EUROCLIMA II
Desertification, Land Degradation and Drought (DLDD), and
bio-physical modeling for crop yield estimation in Latin
America under a changing climate

Deliverable No. 7

Contents

1	Executive Summary	1
2	Introduction to Drought Risk	3
3	Modeling the Determinants of Drought Risk	5
3.1	Drought Hazard	5
3.1.1	The hazard model	5
3.1.2	The precipitation dataset	7
3.2	Drought Exposure	8
3.2.1	Compensatory and non-compensatory models of drought exposure	8
3.2.2	Geographic layers of population, livestock, agriculture and water stress	10
3.3	Drought Vulnerability	11
3.3.1	Social, economic and physical factors of drought vulnerability	11
3.3.2	National and sub-national indicators of vulnerability	13
4	Computation and validation of drought exposure and vulnerability models	14
4.1	Minimum Mapping Unit of Analysis and Geographic Generalization of Indicators	14
4.2	Excluding Countries and other Official Territories	14
4.2.1	Masking very arid and extremely cold regions	15
4.3	Normalization of indicators	16
4.4	Sensitivity analysis and model selection criteria	16
5	Results and Discussion	18
5.1	Drought Hazard	18
5.2	Drought Exposure	19
5.3	Drought Vulnerability	23
5.4	Drought Risk	25
6	Conclusions	28

List of Figures

3.1	Computation of thresholds of monthly drought onset: (1) estimation of the median monthly precipitation totals from an historical time series; (2) “Fisher-Jenks” optimization of the drought threshold level for January; and (3) standardized drought threshold levels optimized for representative months in Latin America.	6
3.2	Onset and end of a drought event.	6
3.3	The computation of drought hazard: (left) number of drought events for Latin America in the period between 1902-2010; (right) probability of exceedance the median global drought severity for two grid points in the region.	7
3.4	Computation of a performance frontier in a simulated Data Envelopment Analysis (DEA) for six regions and two indicators.	9
3.5	Vulnerability factors and possible levels of interaction. Adapted from [1].	11
4.1	Excluded sub-national regions: green areas.	15
4.2	Mask of very arid and extremely cold regions: red areas.	16
5.1	Global map of drought hazard.	18
5.2	World map of the FAO aridity index for 1981-2010, as presented in [2].	19
5.3	Correlation analysis of exposure values computed with (red) compensatory; and (green) non-compensatory approaches: (a) model values as function of maximum indicators’ inputs per sub-national region; (b) non-compensatory model values as function of compensatory model values per sub-national region.	20
5.4	Global map of drought exposure.	21
5.5	Latin American map of drought exposure.	22
5.6	Vulnerability to drought at sub-national regions ordered by the median ensemble rank: (black vertical lines) range of ensemble rank values; (red dots) rank of sub-national regions based on the model with maximum distance to median rank; (green dots) rank of sub-national regions based on the model with minimum distance to median rank.	24
5.7	Global maps of drought vulnerability factors computed with the DEA approach.	26
5.8	Global map of drought vulnerability.	27
5.9	Global map of drought risk.	27

List of Tables

3.1	Indicators of drought vulnerability in detail: corresponding factors, data sources, reference dates and correlation to the overall vulnerability.	13
5.1	Sub-national regions with the highest compensatory drought exposure values and respective: non-compensatory exposure values and normalized indicators' values.	21
5.2	Mean distance of sub-national ranks to the median sub-national rank of the ensemble computed with different vulnerability models.	23
5.3	Indicators of physical factors for illustrative sub-national regions and respective vulnerability values computed models of average combination of non-compensatory (<i>anCompVuln</i>) and compensatory (<i>aCompVuln</i>) aggregation of indicators. . . .	25

1 Executive Summary

This Technical Report was developed in the framework of Component 3 of the second phase of the Programme EUROCLIMA: “Sustainable Agriculture, Food Security and Climate Change in Latin America: Strengthening the capacities of key stakeholders to adapt agriculture to climate change and mitigate its effects”. EUROCLIMA is a regional cooperation program between the European Union and Latin America that focus on climate change and was funded by DG DEVCO/G3. It aims at facilitating the integration of mitigation and adaptation strategies into climate change public policies and development plans in Latin America. In the framework of EUROCLIMA, DG DEVCO established an Administrative Arrangement (AA) with the JRC (No. 2013/332-909, Jan. 2014 – Jan. 2017) to work on the topics of Desertification, Land Degradation and Drought (DLDD), as well as on bio-physical modeling for crop yield estimation in Latin America.

The contents reported in this document correspond to the Deliverable No. 7 of the AA established between DG DEVCO and the JRC. This deliverable focused on the development of models to map the geographic distribution and intensity of drought hazard, exposure, vulnerability and risk for Latin America. Since absolute intensity of risk and its determinants is difficult to quantify, here we focus on models of relative/standardized intensity, where each country (or sub-national administrative region, or local area) is compared with each other and ranked according to some predefined or empirically determined benchmark derived from the environmental, physical, economic and social characteristics of the analyzed regions. Moreover, since the approach is relative and Latin America is part of a global community that interact, share and support each other social, economic and physically, we decided also to conduct our analysis from a global to a continental perspective (in order to place Latin America in the globe), and finally to look at the national and sub-national scales of risk and its determinants in Latin America.

Maps of drought risk have been elaborated at the sub-national level. To the best of our knowledge, this is the first comprehensive and very detailed approach proposed in the literature. Drought risk is computed as the the combination of three determinants, namely: hazard, exposure and vulnerability. The calculation of drought determinants is also new and innovative. Each determinant is calculated independently of each other and based on indicators of different spatial resolutions. The major challenges were: the definition of a standard and effective Minimum Mapping Unit (MMU) of analysis for deriving the final maps; the identification of a general reference date; the selection, collection, and pre-processing of indicators, including normalization to the same max-min range; the aggregation judgment and final combination of indicators.

Drought hazard was computed at the 0.5°. This determinant is based on the non-parametric analysis of historical sequences of monthly precipitation deficits for the period between 1901-2010. Precipitation totals are provided by the Global Precipitation Climatology Centre (GPCC) through the free Full Data Reanalysis Version 6.0 gridded dataset. Drought hazard is estimated for each grid point as the probability of exceedance the median global drought severity for the period of analysis.

Drought exposure is computed at the sub-national level. It is based on spatially generalized very high spatial resolution gridded indicators of population, agriculture, livestock and water stress. The computation of exposure was based on a non-compensatory aggregation of indicators by means of a non-parametric approach, namely the Data Envelopment Analysis (DEA). DEA is a cost-effective means of screening the multivariate distribution of individual input indicators to ensure that potential exposure is identified and its values are robust enough to provide a regional rank that meets the worst-case conditions for timely warning and effective prevention of possible disasters.

Drought vulnerability is derived from the arithmetic combination of high level factors of social, economic and physical indicators, collected both at the national level and gridded layers of very high spatial resolution. It is important to note that each factor is categorized by a single explanatory value that is derived from multiple indicators, which are up- or down-scaled to the

sub-national level and aggregated by means of a DEA model. The proposed 2-step approach for deriving regional drought vulnerability follows the concept that people require a range of “(semi-)independent” factors (characterized by a set of indicators) to achieve positive resilience to impacts and that no single factor on its own is sufficient to yield all the many and varied livelihood outcomes that people need to ensure survival.

While drought hazard has been computed on a method recently proposed at the JRC, several approaches to the computation of drought exposure and vulnerability were needed to be formulated, computed and compared by means of statistically sound techniques based on internal validation judgments. The final selected models have the required statistical properties and the spatial distribution of computed determinants match the overall patterns of elements at risk and the propensity to drought impacts at the expected regions.

The proposed methodologies are robust, consistent, and accurate from the statistical viewpoint. Nevertheless, it is important to highlight that the proposed approaches are fully data driven and the final results can be biased by the uncertainties of input indicators and propagation errors from their combination and aggregation. Although this is a very important point concerning the quality of the final products derived with the proposed methodology, the accuracy assessment of input indicators is out of the scope of this work and the methodological formulation and development of drought risk and its determinants is independent of it.

2 Introduction to Drought Risk

Drought is a recurring and extreme climate event that is originated by a temporary water deficit and may be related to a lack of precipitation, soil moisture, streamflow, or any combination of the three taking place at the same time. The immediate consequences of short-term (i.e. a few weeks duration) droughts are, for example, a fall in crop production, poor pasture growth and a decline in fodder supplies from crop residues, whereas prolonged water shortages (e.g. of several months or years duration) may, among others, lead to a reduction on hydro-electrical production and an increase of forest fire occurrences [3].

Drought is a complex process to model as it is not clear when it starts both in spatial and temporal terms [4]. The same deficit in precipitation may not induce similar impacts depending on types of soil, vegetation and agriculture as well as on differences in irrigation infrastructures [5] [6] [7]. Moreover, casualties are not directly induced by physical drought but rather by food insecurity which is not purely a natural hazard as it includes human induced causes (such as conflicts, poor governance, etc.). However, a generic and comprehensive global approach to drought risk management is nowadays critical for many regions in the world that have a strong dependency on rain-fed agriculture and are affected by food insecurity, such as at several Asian, African and South-Central American countries. Moreover, these regions depend on hydroelectricity and biomass as main sources of energy and droughts directly impact on their economic and social development [8]. In the case of rich nations, drought also poses a big challenge to risk managers, as it: arouses groundwater contamination, leads to an exhaustion of water supplies supporting large scale industry, degrades landscape functioning, limits transportation and diminishes tourism and recreation, raises conflicts over environmental issues such as the protection of catchments, and reduces reservoir capacity for serving growing urban populations [9].

Drought risk is the probability of harmful consequences, or expected losses resulting from interactions between drought hazard (i.e. the possible future occurrence of drought events or rareness of a single event), drought exposure (i.e. the total population, its livelihoods and assets in an area in which drought hazard events may occur), and drought vulnerability (i.e. the propensity of exposed elements to suffer adverse effects when impacted by a drought event) [10]. As drought hazard is increasing globally due to anthropogenic warming activities and certain tasks, such as distributive policies (e.g. relief aid, regulatory exemptions, or preparedness investments), require information on drought exposure and vulnerability comparable across different climatic regions, greater attention has been directed recently to the development of methods for standardized quantification of drought risk [7].

In this study we, therefore, concentrate on a methodology for mapping the global distribution of drought risk, based on the combination of independent indicators of historical drought hazard and current estimates of drought exposure and vulnerability, as previously suggested by [11] and [12]. Drought risk is computed as [13]:

$$\mathbf{Risk} = \mathbf{Hazard} \times \mathbf{Exposure} \times \mathbf{Vulnerability} \quad (2.1)$$

The hazard drought model considers the historical distribution of standardized precipitation deficits, namely their frequency, duration and severity for a region. Since precipitation is the primary variable limiting the water available to the coupled human-environment system, then it is considered as the main factor of drought hazard. To compute hazard, we use a new Meteorological Drought Severity Index (MDSI) [14]. The MDSI is standardized in space and time, and considers the relative monthly precipitation deficits and the seasonal influence of precipitation regimes to meteorological drought severity computation. The motivation for using the MDSI is twofold:

1. the observation that primitive indices of drought severity directly measure local precipitation shortages and cannot be compared geographically; and that

2. standardized indices of drought do not take into account the intra-annual variability of precipitation in estimating the severity of events that can impact on seasonal activities.

Exposure to some natural hazard may be described as “being in the wrong place at the wrong time” [1]. In the case of drought, exposure is determined by several indicators, such as population and livestock density, exploitation of land for agriculture, as well as water withdrawals for domestic and industrial sectors, to cite but a few. The major challenge is to define whether values of one indicator can be traded for values of another indicator in the model configuration or not. Usually, exposure to drought concentrates on life losses and the model is simplified to the ordered rank of one simple indicator for regional comparisons, e.g. [15]. Here we propose a multivariate model that is built on both available and newly created spatially continuous global datasets.

The central function of vulnerability analysis is to identify territories where people will be most dramatically affected by a drought and to analyze the reasons why these groups are less able than others to cope with the impact of the hazard [16]. Therefore, the definition of vulnerability to drought being adopted in this work is similar to the developments of [17] and reflects the complex interactions between social (e.g. education, health) and financial (e.g. energy consumption, poverty headcount ratio) factors assessed at the national scale, as well as a physical factor (e.g. infrastructures such as roads and irrigation mechanisms) mapped at the sub-national scale.

This technical report describes the data sources and calculations for Global Drought Hazard, Exposure, Vulnerability and Risk Mapping. It includes the steps of data collection, pre-processing, models formulation, validation and testing.

3 Modeling the Determinants of Drought Risk

The term risk refers to the expected losses from a particular hazard to a specified element at risk in a particular future time period [18]. “Losses may be estimated in terms of human lives, or buildings destroyed or in financial terms” [13] [19]. There are different challenges when comparing risk levels for different regions, e.g. how to compare large regions with small ones, or how to compare regions affected by earthquakes and those affected by droughts? Because of the specific nature of each hazard type (rapidity of onset, spatial extent and destruction potential), exposures to different hazard types cannot be easily compared. Being affected by drought differs drastically from being exposed to earthquakes. In the first case, infrastructures generally do not suffer, the impact is slow and gradual, but the duration is long, while the inverse is true for earthquakes. Standard and comparable models of hazard, exposure, vulnerability and risk to drought at the sub-national level have been estimated globally by means of statistical analyzes and Geographical Information Systems (GIS) techniques that are presented in this section.

3.1 Drought Hazard

3.1.1 The hazard model

The hazard occurrence at a given location refers to the frequency or returning period of the hazard at a given magnitude [18]. Here, drought hazard is computed as the probability of exceedance (P_e) the median severity of global historical drought events, where $P_e = 1 - P_c$, and P_c is the probability of non-exceedance the median severity of global historical drought events at a given location. The computation of drought hazard follows a four-stage process [14]:

1. For every month and geographic location, the non-parametric “Fisher-Jenks” algorithm is used to estimate a threshold level that optimizes the partition of historical precipitation data observations below the median into j categories of “drought” and “non-drought” (Figure 3.1). Whereas the median of historical precipitation observations is the “best guess” of unknown “normal” climatological precipitation conditions for each month and location, 0 corresponds to the most extreme deficit that can be verified at any time and location [7]. The “Fisher-Jenks” method aims at estimating a monthly threshold value, $PrcThr_m$ ($1 \leq m \leq 12$ months), that minimizes the sum of absolute precipitation deviations about the gravity center of each j category. $PrcThr_m$ is defined in the range between 0 and the median of historical monthly precipitation, Prc_m , and as is computed as follows:

$$\sum_{j=1}^k \sum_{n=1}^{N_{m,j}} |Prc_{m,n,j} - Prc_{m,j}|, \quad (3.1)$$

where $N_{m,j}$ = total number of years with precipitation observations below the median of month m and classified in category j ; $Prc_{m,n,j}$ = precipitation observation in category j , year n and month m ; and $Prc_{m,j}$ = median of monthly precipitation observations m in category j .

2. In the sequence, for each month m in year n , relative precipitation deficits, ΔPrc_t , within the range 0 – 1, are computed as follows:

$$\Delta Prc_t = \begin{cases} \frac{PrcThr_m - Prc_{m,n}}{PrcThr_m} & \text{if } Prc_{m,n} < PrcThr_m \\ 0 & \text{if } Prc_{m,n} \geq PrcThr_m \end{cases}, \quad (3.2)$$

A drought starts at month m and year n if $Prc_{m,n} < PrcThr_m$ (red open circles in Fig. 3.2); if $Prc_{m,n} = 0$ then $\Delta Prc_t = 1$ and the relative monthly precipitation deficit is

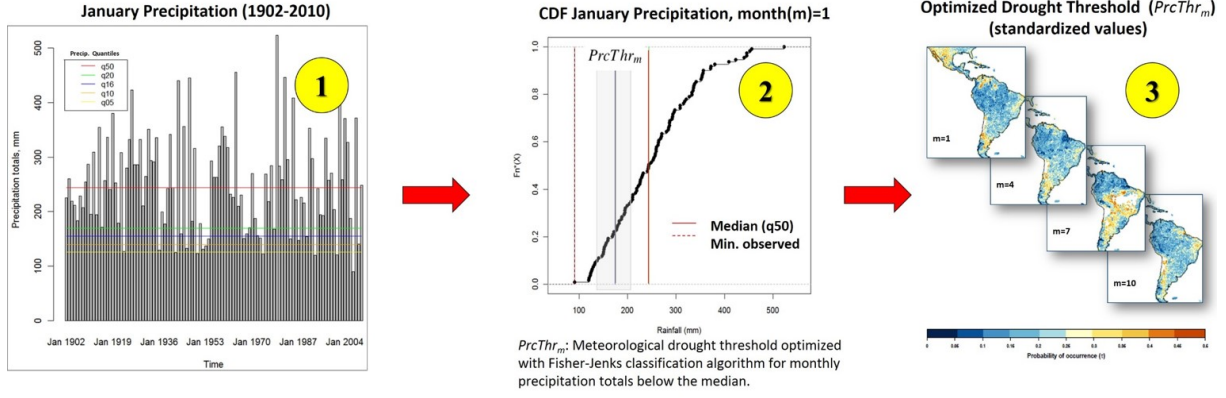


Figure 3.1: Computation of thresholds of monthly drought onset: (1) estimation of the median monthly precipitation totals from an historical time series; (2) “Fisher-Jenks” optimization of the drought threshold level for January; and (3) standardized drought threshold levels optimized for representative months in Latin America.

maximum (not shown in Fig. 3.2); if $Prc_{m,n} \geq PrcThr_m$ then $\Delta Prc_t = 0$ and monthly precipitation totals are within the normal climatological conditions for the region (blue open circles in Fig. 3.2).

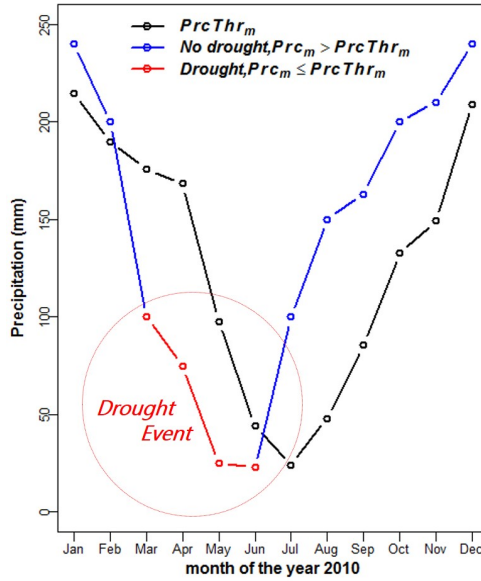


Figure 3.2: Onset and end of a drought event.

- The next step is the calculation of the Meteorological Drought Severity Index (MDSI) [14] for all droughts that occurred worldwide in a specified historical period, as follows:

$$MDSI = \sum_{t=\{n,m\}_o}^{\{n,m\}_e} \Delta Prc_t \times W_m, \quad (3.3)$$

where $\{n,m\}_o$ and $\{n,m\}_e$ are, respectively, the onset and end months of a drought period (March and June in Fig. 3.2). In the case presented in Fig. 3.2, $\{n,m\}_o = March, 2010$ and $\{n,m\}_e = June, 2010$. W_m is a variables that compensates for the differences in the absolute amount of monthly precipitation deficits in regions with recurring dry and/or wet

seasons. It is used to give more influence to the annually recurring period(s) of one or more months when most of precipitation occurs. W_m standardizes the relative monthly precipitation deficits for the computation of drought severity for each location and is defined as follows:

$$W_m = \frac{PrcThr_m}{\sum_{m=1}^{12} PrcThr_m}. \quad (3.4)$$

where by definition: $W_m \geq 0$ and $W_1 + W_2 + \dots + W_{12} = 1$. The practical use of W_m is illustrated for the case presented in Fig. 3.2: for the same ΔPrc_t , the month of March has an influence larger than June on drought severity because $W_3 = 0.14 \gg W_6 = 0.04$.

4. Finally, for each geographic location, drought hazard is computed by comparing the Global and Local Empirical Cumulative Distribution functions (ECDFs) of drought severity for $p(\overline{MDSI}_{global})$ and estimating $P_e = 1 - P_c$, as present in Fig. 3.3 for Latin America.

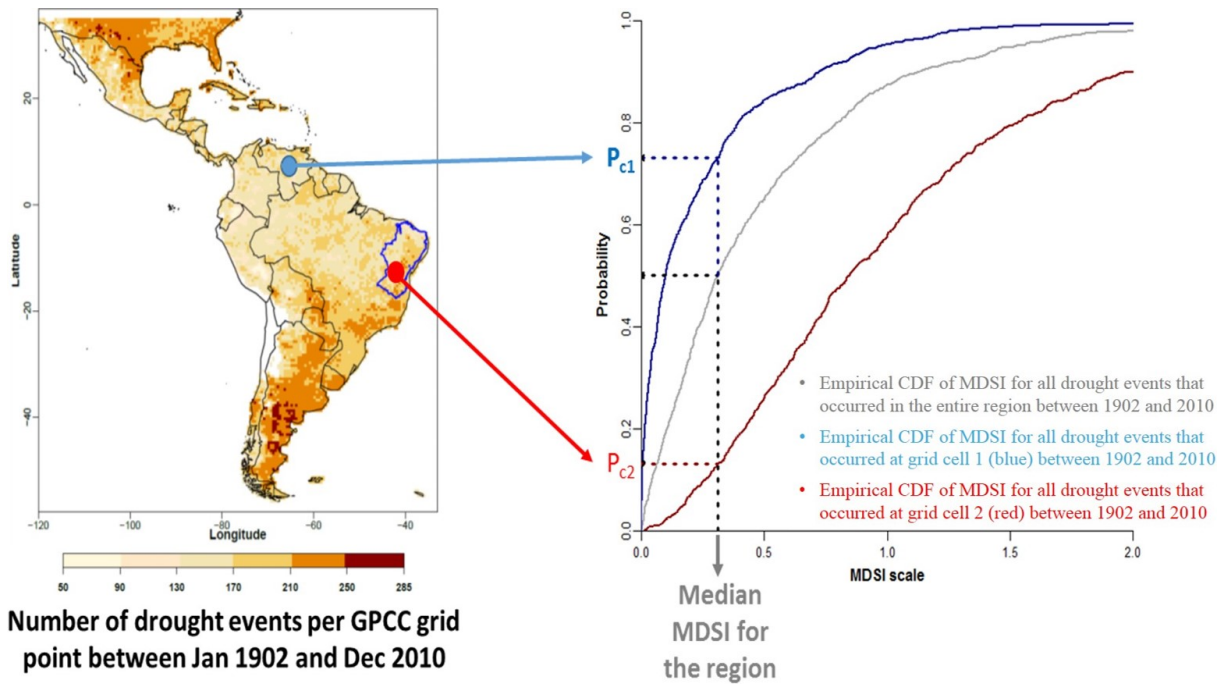


Figure 3.3: The computation of drought hazard: (left) number of drought events for Latin America in the period between 1902-2010; (right) probability of exceedance the median global drought severity for two grid points in the region.

3.1.2 The precipitation dataset

The calculation of drought hazard is performed with monthly precipitation totals from the global free gridded dataset Full Data Reanalysis Version 6.0 provided by the Global Precipitation Climatology Centre (GPCC) of the German Weather Service (Deutscher Wetterdienst, DWD [20]. This choice is based on three main reasons: first, it is a spatially interpolated dataset based on the highest number of collected precipitation records; second, it spans from January 1901 to December 2010 and all grid points have no missing data after January 1951; third, this dataset has been used in many drought-related studies from regional to global scales.

Version 6.0 is based on the merging of data series from rain-gauges built from Global-Telecommunication-System-based data and historic data records. The dataset comprises a world-wide total of more than 67,000 stations that feature record durations of at least 10 years

or longer. It contains the monthly precipitation totals on regular grids with a spatial resolution of $0.5^\circ \times 0.5^\circ$, $1.0^\circ \times 1.0^\circ$, and $2.5^\circ \times 2.5^\circ$. The high-resolution monthly product ($0.5^\circ \times 0.5^\circ$) was selected for the analysis, since it allows better analyzing the regional drought patterns. Some problems were found in the regions with less data coverage, namely Greenland, Arctic areas, Sahara Desert, Tibetan Plateau, Mexico and high-elevation points in Chile. However, the outliers were extremely rare ($< 0.15\%$).

3.2 Drought Exposure

Drought exposure is derived from the combination of a set of quantitative indicators mapping the distribution of population and assets or goods that can be affected by both short- and long-term drought events. In this work, a special attention is given to agricultural assets, as these are highly dependent of precipitation availability and short-term deficits can seriously damage crop production. Nevertheless, other sectors of activity, such as water consumption for livestock production and industrial water pressure are also considered. The exposure of ecological units or natural habitats is not foreseen in this compendium.

3.2.1 Compensatory and non-compensatory models of drought exposure

When developing a model of exposure to drought based on the combination of a set of simple indicators, two types of judgment can be considered and tested: compensatory or non-compensatory [21]. A compensatory or non-compensatory distinction can be made on the basis of whether values of one indicator can be traded for values of another indicator in the model configuration or not. For more details see, e.g. the following notes:

<https://www.youtube.com/watch?v=CKM9u65kZHg>

<http://www.deafontier.net/deaintro.html>

<http://www.mycbbook.com/MYCBBook-Consumer-Decision-Judgment-Models.pdf>

In a compensatory model, drought exposure is ranked by considering all of the indicators' values and by trading off the region's high value on one or more indicators with its lower values on other indicators. Most common compensatory models are based on additive methods, such as the simple sum or average of input indicators, as follows [17]:

$$CompExp = \sum_{i=1}^n Ind_i \times W_i , \quad (3.5)$$

where W_i is the weight assigned to indicator Ind_i (with $\sum W_i = 1$). These models are compensatory because a shortfall on one indicator may be compensated by an high value on other indicator.

When a set of indicators are used to evaluate the exposure to drought on a set of regions, some may be in favor of one particular region, while others will favor another. As a consequence, a conflict among the indicators could arise. For example, a region might be 100% covered by rainfed crops with no livestock or population being set there. In the non-compensatory model a superiority in one indicator cannot be offset by an inferiority in some other indicator(s). In words, we consider that a region is highly exposed to drought if at least one of the assets is highly represented there. In the compensatory model, a region would attain maximum exposure only in the case that it was entirely occupied by agriculture and at the same time being the most populated area and larger livestock producing region in the world. This is physically impossible. Therefore, in a non compensatory approach each indicator stands on its own and a conflict can be easily treated by taking into account the absence of preferential independence within a discrete multi-criteria approach. Among different non-compensatory methods, Data Envelopment Analysis (DEA) [22] [23] is a non-parametric approach that can be used for estimating an

efficiency multidimensional frontier of maximum drought exposure in the sample dataset and to measure the relative exposure of different regions to drought. The following assumptions are made for DEA benchmark and ranking [24]:

- The higher the value of a given indicator, the more exposure for the corresponding region;
- Non-discrimination of regions that are the most exposed in a single indicator, thus ranking them equally;
- A linear combination of the best performers is feasible, i.e. convexity of the frontier.

The relative exposure of each region with respect to the benchmark of maximum exposure to drought in the sample dataset, is determined by the location of the region and its multidimensional distance relative to the DEA frontier. Both issues are represented in Figure 3.4 for the simple case of six regions (P_1, P_2, \dots, P_6) and two abstract indicators (y_1 and y_2) that are represented in the two axes. Regions will be ranked according to their score in each of the indicators. The line connecting countries P_1, P_2, P_3 and P_4 (that has been notionally extended to the axes by the lines “ P_1y_2' ” and “ P_4y_1' ” to enclose the entire dataset) constitutes the performance frontier (i.e. maximum exposure among the regions represented in the dataset) and the benchmark for regions P_5 and P_6 which lie below that frontier. The countries supporting the frontier are classified as the most exposed according to their values in both axes. The most exposed regions will have a performance score of 1, while regions P_5 and P_6 , which are within this envelope, are less exposed than the others and score values between 0 and 1.

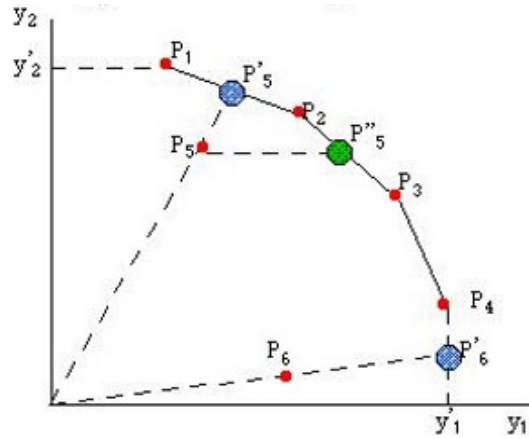


Figure 3.4: Computation of a performance frontier in a simulated Data Envelopment Analysis (DEA) for six regions and two indicators.

The non-compensatory exposure values can be computed with DEA for regions P_5 and P_6 , as follows [24]:

$$nCompExp = \overline{0P_j} / \overline{0P'_j} , \quad (3.6)$$

where $\overline{0P_j}$ is the multivariate distance between the origin and the actual observed region j , and $\overline{0P'_j}$ is the distance between the origin and the projected region in the frontier of maximum exposure. The exposure value for these regions depends on their position with respect to the frontier, while the benchmark will correspond to the worst situation according to the values of the other regions measured in the set of the same indicators. $\overline{0P'_j}$ is always estimated as the shortest distance between the origin and the frontier when crossing P_j . In the example shown in Figure 3.4, the distance from the origin to P'_5 is shorter than that to $P''5$ and is the one considered by DEA for computing the respective exposure, as shown in Figure 3.4.

3.2.2 Geographic layers of population, livestock, agriculture and water stress

Compensatory and non-compensatory models of drought exposure will be computed on the basis of four geographic layers that completely cover the global land surface. These layers are:

- **Population Count**

- *Description:* The population count grid, consists of estimates of the number of persons per 30 arc-second grid cell for 2010.
- *Authors:* Balk, D.L., U. Deichmann, G. Yetman, F. Pozzi, S.I. Hay, and A. Nelson.
- *Title of publication:* Gridded Population of the World, Version 4 (GPWv4), Preliminary Release 2.
- *Year of publication:* 2014.
- *URL:* <http://www.ciesin.columbia.edu/data/gpw-v4>.
- *Resolution:* 30 arc-second raster (about 1x1 km at the equator).

- **Gridded Livestock of the World (GLW)**

- *Description:* Modelled livestock densities of the world, adjusted to match official (FAOSTAT) national estimates for the reference year 2005.
- *Authors:* Timothy P. Robinson, G. R. William Wint, Giulia Conchedda, Thomas P. Van Boeckel, Valentina Ercoli, Elisa Palamara, Giuseppina Cinardi, Laura DAietti, Simon I. Hay, Marius Gilbert.
- *Title of publication:* Mapping the Global Distribution of Livestock.
- *Year of publication:* 2014.
- *URL:* [doi:10.1371/journal.pone.0096084](https://doi.org/10.1371/journal.pone.0096084).
- *Resolution:* 3 arc minute raster (about 5x5 km at the equator).

- **Global agricultural land cover data set**

- *Description:* Estimated percentage of surface land covered by croplands and pastures circa 2000, derived from automatic classification of satellite-derived data and agricultural inventory data.
- *Authors:* Navin Ramankutty, Amato T. Evan, Chad Monfreda, and Jonathan A. Foley.
- *Title of publication:* Farming the planet: 1. Geographic distribution of global agricultural lands in the year 2000.
- *Year of publication:* 2008.
- *URL:* [doi:10.1029/2007GB002952](https://doi.org/10.1029/2007GB002952).
- *Resolution:* 5 arc minute raster (about 10x10 km at the equator).

- **Baseline Water Stress**

- *Description:* Total annual water withdrawals (municipal and industrial) expressed as a percent of the total annual available flow; higher values indicate more competition among users.
- *Authors:* Gassert, F., M. Landis, M. Luck, P. Reig, and T. Shiao.
- *Title of publication:* Aqueduct Global Maps 2.1. Working Paper.
- *Year of publication:* 2014.
- *URL:* <http://www.wri.org/publication/aqueduct-metadata-global>.
- *Resolution:* Hydrological catchment.

3.3 Drought Vulnerability

The last determinant of drought risk, vulnerability, is less easily apprehended. Vulnerability depends critically on the context of the analysis, and the factors that make a system vulnerable to a natural hazard will depend on the nature of the system and the type of hazard in question. The factors that make a rural community in semi-arid Africa vulnerable to drought will not be identical to those that make areas of a wealthy industrialized nation, such as Norway, vulnerable to flooding, wind storms and other extreme weather events. Nonetheless, there are certain factors that are likely to influence vulnerability to some specific hazard in different geographical and socio-political contexts [25]. These are developmental factors including indicators such as poverty, health status, economic inequality and elements of governance, to cite but a few. Although the relative importance of different factors will exhibit some geographic variation, such factors may be viewed as the foundation of specific measures for reducing vulnerability and facilitating adaptation to drought.

3.3.1 Social, economic and physical factors of drought vulnerability

To compute a global map of drought vulnerability, we followed a framework similar to the UN International Strategy for Disaster Reduction (UN/ISDR) [1], where this determinant of risk is a reflection of the state of the individual and collective physical, social and economic conditions of a region at hand. Figure 3.5 illustrates the three broad factors in which different aspects of vulnerability can be grouped, depicted by intersecting circles to show that all spheres interact with each other.

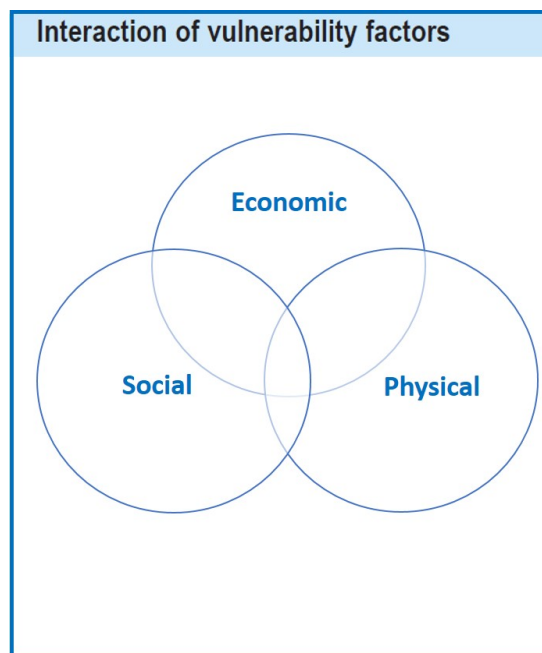


Figure 3.5: *Vulnerability factors and possible levels of interaction. Adapted from [1].*

The framework proposed by [1] considers each factor as an individual dimension that reflect the essential conceptual aspects of a civil society and can be used independently as a guidelines to stakeholders, policymakers and practitioners alike. The adopted approach allows the evaluation of the strengths and weaknesses of each factor to the total vulnerability score in a region. Social vulnerability is linked to the level of well-being of individuals, communities and society; economic vulnerability is highly dependent upon the economic status of individuals, communities and nations; physical vulnerability comprises the basic infrastructures needed to support the production of goods and sustainability of livelihoods [26].

Vulnerability to drought is computed based on a 2-step composite indicator that derives from the aggregation of indicators characterizing the three factors previously indicated in Figure 3.5: economic, social and physical. In the first step, indicators for each factor are combined using, for example, compensatory or non-compensatory approaches, as previously discussed in sub-section 3.2. In the second step, individual factors are aggregated into a composite index of vulnerability by using, e.g. a geometric mean (as similar as to the Human Development Index [27]), a weighted arithmetic mean (as similar as to the Drought Vulnerability Index (DVI) [17]) or the product (as similar as to Multidimensional Poverty Index (MPI) [28]). In this report, we formulate, evaluate and select a combined indicator of vulnerability to drought by testing and comparing eight different composite schemes, as follows:

1. Compensatory Average model of indicators within each factor:

a) Geometric aggregation of factors:

$$gCompVuln = \sqrt[3]{\left(\sum_{i=1}^{nSoc} Ind_i \times W_i\right) \times \left(\sum_{i=1}^{nEcon} Ind_i \times W_i\right) \times \left(\sum_{i=1}^{nPhys} Ind_i \times W_i\right)}, \quad (3.7)$$

b) Arithmetic aggregation of factors:

$$aCompVuln = \frac{\left(\sum_{i=1}^{nSoc} Ind_i \times W_i\right) + \left(\sum_{i=1}^{nEcon} Ind_i \times W_i\right) + \left(\sum_{i=1}^{nPhys} Ind_i \times W_i\right)}{3}, \quad (3.8)$$

c) Weighted Arithmetic aggregation of factors:

$$\begin{aligned} waCompVuln = & \left(\sum_{i=1}^{nSoc} Ind_i \times W_i\right) \times (nSoc / (nSoc + nEcon + nPhys)) + \\ & + \left(\sum_{i=1}^{nEcon} Ind_i \times W_i\right) \times (nEcon / (nSoc + nEcon + nPhys)) + \\ & + \left(\sum_{i=1}^{nPhys} Ind_i \times W_i\right) \times (nPhys / (nSoc + nEcon + nPhys)), \end{aligned} \quad (3.9)$$

d) Product aggregation of factors:

$$pCompVuln = \left(\sum_{i=1}^{nSoc} Ind_i \times W_i\right) \times \left(\sum_{i=1}^{nEcon} Ind_i \times W_i\right) \times \left(\sum_{i=1}^{nPhys} Ind_i \times W_i\right). \quad (3.10)$$

2. Non-Compensatory DEA model of indicators within each factor:

a) Geometric aggregation of factors:

$$gnCompVuln = \sqrt[3]{DEAsoc \times DEAecon \times DEAphys}, \quad (3.11)$$

b) Arithmetic aggregation of factors:

$$anCompVuln = \frac{DEAsoc \times DEAecon \times DEAphys}{3}, \quad (3.12)$$

c) Weighted Arithmetic aggregation of factors:

$$\begin{aligned} wanCompVuln = & DEAsoc \times (nSoc / (nSoc + nEcon + nPhys)) + \\ & + DEAecon \times (nEcon / (nSoc + nEcon + nPhys)) + \\ & + DEAphys \times (nPhys / (nSoc + nEcon + nPhys)), \end{aligned} \quad (3.13)$$

d) Product aggregation of factors:

$$pnCompVuln = DEAsoc \times DEAecon \times DEAphys. \quad (3.14)$$

3.3.2 National and sub-national indicators of vulnerability

As mentioned in the previous section, vulnerability to drought is quantified by means of social, economic and physical factors, which indicators are chosen to reflect the level of quality of different constituents of a civil society. Each factor is characterized by a set of simple indicators that are generalized at the national and sub-national scales. Fifteen indicators selected in accordance with the works published by, e.g. [26] [25] [17] and [28], to cite but a few, are distributed among the three factors according to Table 3.1.

Table 3.1: *Indicators of drought vulnerability in detail: corresponding factors, data sources, reference dates and correlation to the overall vulnerability.*

Factors	Indicator	Resolution	Corr	Year	Source ¹
Economic	* Energy Consumption per Capita (Million Btu per Person)	Country	Neg	2011	U.S. EIA
	* Agriculture (% of GDP)	Country	Pos	2005-2014	World Bank
	* GDP per capita (current US\$)	Country	Neg	2005-2014	World Bank
	* Poverty headcount ratio at \$1.25 a day (PPP) (% of population)	Country	Pos	2005-2014	World Bank
Social	* Rural population (% of total population)	Country	Pos	2005-2014	World Bank
	* Literacy rate (% of people ages 15 and above)	Country	Neg	2005-2014	World Bank
	* Improved water source (% of rural population with access)	Country	Neg	2005-2014	World Bank
	* Life expectancy at birth (years)	Country	Neg	2005-2014	World Bank
	* Population ages 15-64 (% of total)	Country	Neg	2005-2014	World Bank
	* Refugee population by country or territory of asylum (%)	Country	Pos	2005-2014	World Bank
	* Government Effectiveness	Country	Neg	2013	WGI
	* Disaster Prevention Preparedness (OECD, DAC), \$ Year/capita	Country	Neg	2005-2014	OECD
Physical	* Agricultural irrigated land (% of total agricultural land)	5 arc minute raster	Neg	2008	FAO
	* % of retained renewable water	Hydrological catchment	Neg	2010	Aquastat
	* Road density (km of road per 100 sq. km of land area)	Vector	Neg	1980 - 2010	gROADSv1

¹Sources:

World Bank, <http://data.worldbank.org/products/wdi>

U.S. Energy Information Administration (EIA), <http://www.eia.gov/>

Worldwide Governance Indicators (WGI), <http://info.worldbank.org/governance/wgi/index.aspx#home>

Organisation for Economic Co-operation and Development (OECD), <http://stats.oecd.org/>

Food Agriculture Organization (FAO), <http://www.fao.org/nr/water/aquastat/main/index.stm>

Aquastat, <http://www.wri.org/our-work/project/aqueduct>

Global Roads Open Access Data Set (gROADSv1), <http://sedac.ciesin.columbia.edu/data/set/groads-global-roads-open-access-v1>

4 Computation and validation of drought exposure and vulnerability models

Several approaches to computing drought exposure and vulnerability were tested and compared in order to select the most reliable model for the estimation of the determinants of risk at the global scale. The approaches tested for computing drought exposure and vulnerability were described, respectively, in subsections 3.2.1 and 3.3. Next, we describe the dataset used to make the minimum mapping unit (MMU) uniform for all geographic layers, the selection process of countries and sub-national regions for the analysis and the normalization of indicators. In the sequence, we describe the methodology used for comparing the models of drought exposure and vulnerability, as well as the criteria for selecting the final approaches.

4.1 Minimum Mapping Unit of Analysis and Geographic Generalization of Indicators

Global models of drought exposure and vulnerability were computed for sub-national administrative regions. There are three main reasons:

- Raster layers of exposure indicators and indicators of physical vulnerability have different spatial resolutions that need to be harmonized to a common MMU. The spatial generalization of these layers to the sub-national administrative regions is applied because it minimizes the propagation of geographic errors from each indicator during the construction of the model;
- Information for administrative regions is easily apprehended and handled by stakeholders and policymakers within drought early warning systems;
- National and international funding for prevention, mitigation and recovery from the impacts of natural hazards are mainly distributed through administrative regions.

To globally summarize the raster values of exposure indicators and indicators of physical vulnerability at the the first level of sub-national administrative regions, we used the Global Administrative Unit Layers (GAUL) Release 2015, an initiative implemented by FAO within the Bill & Melinda Gates Foundation, Agricultural Market Information System (AMIS) and AfricaFertilizer.org projects. The GAUL compiles and disseminates the best available information on administrative units for all the countries in the world, providing a contribution to the standardization of the spatial dataset representing administrative units. The GAUL always maintains global layers with a unified coding system at country, first (e.g. departments) and second administrative levels (e.g. districts). For more information, please visit GAUL online at <http://www.fao.org/geonetwork/srv/en/metadata.show?id=12691>.

4.2 Excluding Countries and other Official Territories

Models of exposure and vulnerability were computed and evaluated on the basis of 170 countries and 2515 sub-national administrative regions (Figure 4.1). Countries, sub-national regions and other official territories were excluded from the analysis if:

- Are not covered by geographic layers of exposure and/or physical vulnerability;
- Are entirely covered by surface water bodies;
- Are not described by social and/or economical indicators of drought vulnerability;
- Are part, commonwealth, territory or dependency of other countries, such as Isle of Man, French Polynesia, or Macao, to cite but a few;

- Are classified as very arid or extremely cold areas - please see subsection 4.2.1;

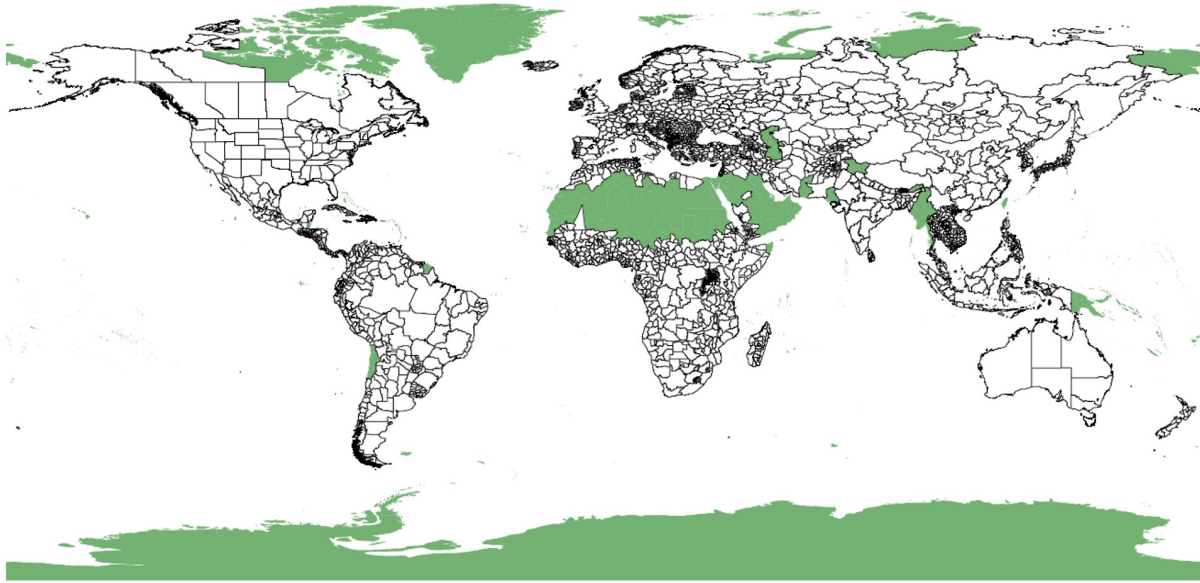


Figure 4.1: *Excluded sub-national regions: green areas.*

4.2.1 Masking very arid and extremely cold regions

Very arid and cold areas were excluded from the computations. It was assumed that dealing with drought concepts in extremely dry regions would be physically meaningless. In order to exclude areas by means of an objective methodology, a combination of conditions derived from three different indicators was used. First, areas where one or more months show more than 25% zero values of cumulated precipitation were excluded. This avoids computing biased SPI-12 records based on Gamma distributions constructed over an insufficient number of values.

Second, the arid areas have been excluded using the FAO Aridity Index (AI [29], computed as the ratio between the annual cumulated precipitation and the annual cumulated evapotranspiration (ET). For simplicity, ET was replaced by potential evapotranspiration (PET). One single AI value, related to the average of sixty annual AI values from 1951 to 2010, was assigned to each grid point. According to the AI classification, global areas are divided into: humid ($AI > 0.75$), sub-humid ($0.65 < AI \leq 0.75$), dry ($0.5 < AI \leq 0.65$), semi-arid ($0.2 < AI \leq 0.5$), arid ($0.05 < AI \leq 0.2$), hyper-arid ($0.03 < AI \leq 0.05$), and desert ($AI \leq 0.03$). Areas with $AI \leq 0.05$ were excluded from the analysis.

Third, the cold areas have been excluded using the annual PET: if the average PET between 1951 and 2010 was smaller than 365 mm, the drought variables for the corresponding grid points were not computed. Moreover, Antarctica was labeled as cold land and cut off from the maps. To calculate PET and consequently AI, we used the CRU TS v3.2 dataset (Climate Research Unit Time Series [30]) of the University of East Anglia. A similar land-masking strategy was used by [31] for drought monitoring based on a special indicator derived from a merging of SPI and SPEI.

While the total emerged lands of the Earth sum up to $148.94 \times 10^6 \text{km}^2$ [32], the presented drought maps take into account approximately $100.35 \times 10^6 \text{km}^2$, which corresponds to 67% of the total emerged lands or to 74% if Antarctica (about $14 \times 10^6 \text{km}^2$) is not considered (Figure 4.2).

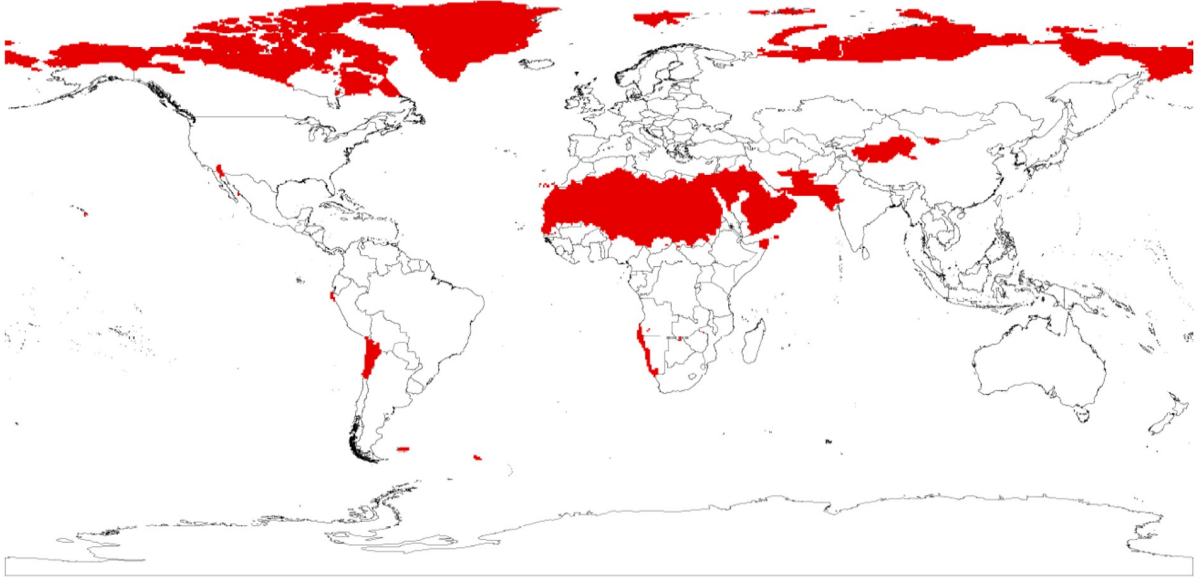


Figure 4.2: Mask of very arid and extremely cold regions: red areas.

4.3 Normalization of indicators

After summarizing raw values of indicators of drought exposure (subsection 3.2.2) and drought vulnerability (subsection 3.3.2) for all sub-national administrative regions of first level, as defined in GAUL and not removed by the process defined in subsection 4.2, we normalized indicators among regions for display and aggregation. The normalization has been made taking into account the maximum and minimum value of each indicator across all regions in order to guarantee that indicators have an identical range between 0 and 1 and the same variance for computing exposure and factors of vulnerability [24]. Regarding indicators of exposure and those with a positive correlation to the overall vulnerability (see Table 3.1), the normalized value is calculated according to the general linear transformation, as follows [17]:

$$Z_i = \frac{X_i - X_{min}}{X_{max} - X_{min}}, \quad (4.1)$$

where X_i represents the indicator value for a generic sub-national region i , X_{min} and X_{max} the respective minimum and maximum value across all regions. In some cases there is an inverse relationship between vulnerability and indicators (e.g. GDP per capita, adult literacy rate, or road density). For indicators with negative correlation to the overall vulnerability (see Table 3.1), a transformation was applied to link the lowest indicator values with the highest values of vulnerability, as follows [17]:

$$Z_i = 1 - \frac{X_i - X_{min}}{X_{max} - X_{min}}, \quad (4.2)$$

4.4 Sensitivity analysis and model selection criteria

A sensitivity analysis was undertaken in order to assess the robustness of the predictive models of drought exposure and vulnerability. Sensitivity analysis is the study of how the uncertainty in the output of a mathematical model or system (numerical or otherwise) can be apportioned to different sources of uncertainty in its inputs, namely indicators, weighting and aggregation schemes [33]. This examination was conducted for the models of drought exposure and vulnerability that were described, respectively, in subsections 3.2.1 and 3.3. The main decisions tested were:

1. Multivariate ranking of exposure and vulnerability factors based on compensatory and non-compensatory judgment of respective indicators;
2. Aggregation of vulnerability factors according to geometrical, arithmetic and product frameworks.

Weighting of factors and indicators was not considered as all indicators and factors are assumed to contribute equally for the respective models. Weights can be better assigned through expert knowledge, which was not part of this global drought risk mapping effort.

The order and stability of exposure and vulnerability rankings assigned by compensatory and non-compensatory judgments and aggregation schemes to a given sub-national administrative region i , respectively denoted by $Rank(ModExp_i)$ and $Rank(ModVul_i)$, are indicators of the robustness of the estimations [17]. For the case of exposure, and as mentioned in subsection 3.2.1, it is expected that an higher value in one indicator cannot be offset by a lower value in some other indicator(s). In other words, we consider that a region is highly exposed to drought if at least one of the assets is highly represented there. Therefore, the selection criteria between compensatory/non-compensatory models of exposure indicators is based on the correlation (ρ) between $Rank(ModExp_i)$ and $\max_i\{Z_{k,i}\}$ as follows:

$$\rho(\max_i\{Z_{k,i}\}, Rank(ModExp_i)) = \frac{\mathbf{Cov}(\max_i\{Z_{k,i}\}, Rank(ModExp_i))}{\sqrt{\mathbf{Var}(\max_i\{Z_{k,i}\})\mathbf{Var}(Rank(ModExp_i))}}, \quad (4.3)$$

where $\{Z_{k,i}\}$ corresponds to the set of k normalized exposure indicators in region i . A larger correlation implies that the model is able to more accurately capture regions of high exposure, independently of being exposed in one, few or many indicators.

Regarding vulnerability, the selection criteria for the best model is internal and based on the minimum distance between each of the regional rankings estimated through the eight models presented in subsection 3.3 and the median regional ranking of the ensemble set defined by the outputs of all models. For example, for model $gCompVuln$ defined in Eq. 3.7, the distance criteria $\bar{R}_{gCompVuln}$ for its evaluation and comparison with the other models is computed as:

$$\bar{R}_{gCompVuln} = \frac{1}{N} \sum_{i=1}^N |medR_i - R_{i,gCompVuln}|, \quad (4.4)$$

where $medR_i$ is the median of the ensemble of ranks computed for region i with all the models presented in subsection 3.3, and $R_{i,gCompVuln}$ is the rank estimated by $gCompVuln$ for the same region i . Among different possibilities, we used the distance to the median baseline scenario for selecting the best model. The median is a non-parametric sample statistic and an unbiased reference of central location for any statistical distribution [34]. We decided to use the median rank of regional vulnerability, instead of the mean, because there are few models available (only 8) to derive parametric sample statistics for each region.

5 Results and Discussion

In this section, we present the global maps for each of the determinants of risk, as well as the results of the sensibility analysis performed for choosing among the best models of drought exposure and vulnerability.

5.1 Drought Hazard

Figure 5.1 shows the world map of drought hazard computed for the events taking place in the period between January 1901 and December 2010. Overall, it is noticeable a match between the geographic distribution of global drought hazard, as computed with the MDSI, and the wide range of global aridity classes, as depicted by the global map of aridity (Figure 5.2) computed with the aridity index classification proposed by [2]. In detail, drought hazard is generally high for semiarid areas, such as Northeastern and Southern South America, Northern, Eastern, Southwestern and Horn of Africa, Central Asia, Australia, West U.S. and the Iberian Peninsula. In opposition, drought hazard is low for tropical regions, such as the Amazon, Central Africa and Southern Asia.

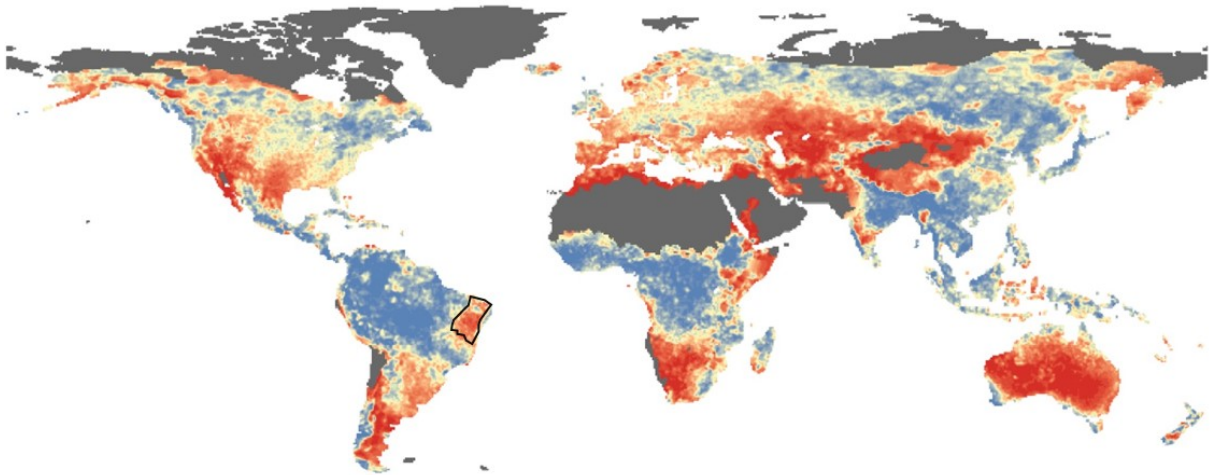


Figure 5.1: *Global map of drought hazard.*

Looking now at the regional scale and the results presented for, e.g. Latin America, the semi-arid region of northeast Brazil, southern Argentina, the Gran Chaco (northern Argentina, southeastern Bolivia and north-western Paraguay), and northeast Mexico are immediately identified as hot spots subject to severe drought conditions, whereas the areas less prone to severe drought conditions match the fully humid areas of north-west Amazon rainforest and the warm temperate climates of southern Chile and south-east Brazil. In general, the spatial consistency of drought hazard patterns with different climate conditions at the regional scale is indicative of the applicability of the index over regions with distinct precipitation regimes.

Let us also look in detail at the link between drought hazard mapped with the MDSI and the drought hazard pattern at the national scale, e.g. the semi-arid spaces of northeast Brazil. In 1936, a section of northeast Brazil was officially recognized by the federal government as having a common recurrence of drought episodes and it was delimited under the name of Drought Polygon to augment the governmental support to the resident populations living there [35] [36]. The initial figure of the Drought Polygon no longer exists and it was substituted by the Semi-Arid Region of the Constitutional Fund for Financing the Northeast Brazil [36]. Currently, the Semi-Arid Region of Northeast Brazil (SARNB) (black polygon in Fig. 5.1) covers 895,254.40 km² and officially delimits the region that is most affected by recurrent severe droughts in the country [36]. The geographic shape of SARNB results from the intersection of three distinct

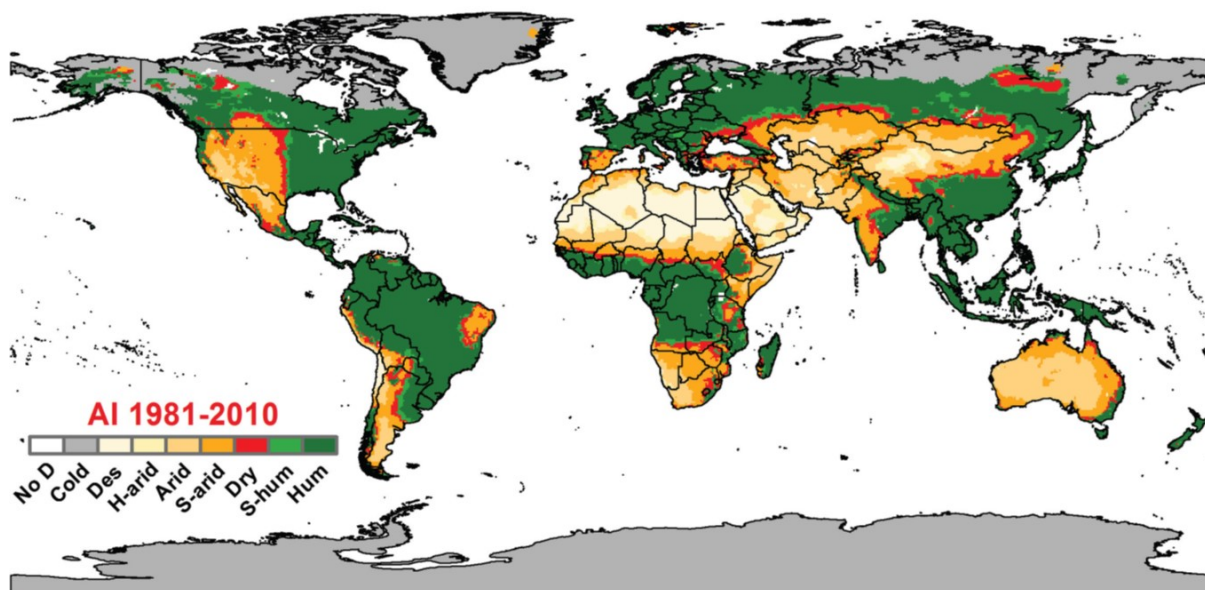


Figure 5.2: World map of the FAO aridity index for 1981-2010, as presented in [2].

climate criteria, namely [36]: (a) mean annual precipitation inferior to 800 *mm*; (b) aridity index value inferior to 0.5 (as defined by [29] and computed from the climatological precipitation and potential evapotranspiration normals between 1961 and 1990); and (c) more than 60% of days under soil moisture deficit between 1970 and 1990 (computed with a daily model of soil water balance that includes precipitation, evapotranspiration and soil parameters). The results shown in Fig. 5.1 confirm that the geographic distribution of the drought hazard computed with MDSI for northeast Brazil is overall consistent with the geometric shape of SARNB. The exceedance probability of severe drought events inside the SARNB is at least double the corresponding percentage in its vicinity (between 20 – 75% inside and $\leq 10\%$ outside). These results seem to emphasize the validity of MDSI and lend additional support to its use for estimating drought hazard from national to global scales. Since the MDSI is standardized and only based in monthly precipitation totals, it is useful to compare drought hazard across different climatic regions and time periods.

Since available water resources in semiarid areas are often insufficient to permanently meet the demands of human activities, these outcomes highlight the aggravated risk for food security and confirm the need for the implementation of drought mitigation and adaptation measures in those regions. Nevertheless, but interestingly though, is the fact that some humid areas in wealthy regions, such as Northwest France, Southeast England, Southeast Brazil, Uruguay, and Southeast U.S., which are extensively exploited for agriculture and livestock production, show some moderate drought hazard that must be monitored as future trends show an increase of drought frequency and intensity for these regions [37].

5.2 Drought Exposure

Two modeling approaches for computing a global map of drought exposure were tested: (1) compensatory; and (2) non-compensatory. A correlation analysis was done with the maximum of the four normalized exposure indicators per sub-national region and the outputs of models (1) and (2) to analyze how individual indicators were contributing to the distribution of overall exposure values. The results presented in Figure 5.3 (a) show a good agreement between the maximum value of normalized indicators per sub-national region and the outputs of both models, with correlation coefficients of 0.96 and 0.99 for compensatory and non-compensatory approaches, respectively, at the 5% significance level.

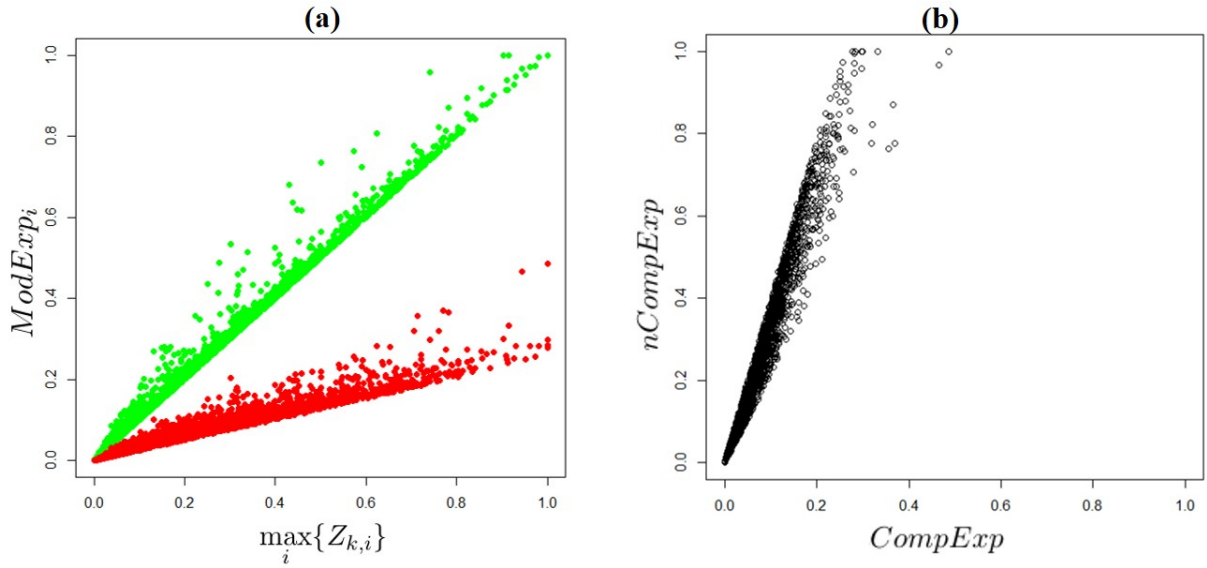


Figure 5.3: Correlation analysis of exposure values computed with (red) compensatory; and (green) non-compensatory approaches: (a) model values as function of maximum indicators' inputs per sub-national region; (b) non-compensatory model values as function of compensatory model values per sub-national region.

Since correlation values are positive, these results demonstrate that as long as the values of at least one exposure indicator increase, exposure will increase as well from both models. Nevertheless, and although both models show a very high positive correlation with the maximum value of the four normalized indicators, the results from Figure 5.3 (b) highlight the fact that the compensatory approach minimizes the variability of exposure values to the interval $[0, 0.5]$. These results support the idea that low values in one or more indicators will reduce regional exposure, even if the values for the remaining indicators are high.

To analyze the discourse of the previous paragraph, let us look in detail at the numbers in Table 5.1. The rows of the table are representative of the 17 sub-national regions with the highest compensatory drought exposure values, and are ranked by their descending order (column "C"). The detailed analysis of the values in Table 5.1 shows that the compensatory model suffers from a number of pitfalls: as it assumes that low values in one or more indicators counterbalance the high values on other indicators, it lessens regional exposure and smooths the regional variability from input indicators. Therefore, the compensatory approach does neither guarantee the representation of regional extreme exposure values, nor the absolute contribution of single indicators to final regional exposure. Let us look in detail, for example, at Dki Jakarta region, Indonesia. Although worldwide this is the region with the highest population density (as mapped by the GPWv4 dataset, subsection 3.2.2), its compensatory exposure value is almost half of that for Rangpur region, Bangladesh, which is characterized by the highest percentage of territory covered by agriculture. The compensatory approach considers that Dki Jakarta is less exposed because only one indicator is showing high values, i.e. population density, whereas Rangpur region has also a high livestock production. As discussed before, a continuous urban area cannot be highly covered by agriculture nor simultaneously accommodate infrastructures for high livestock production, but it is still extremely exposed because the number of people living there is comparatively high to that of other regions. On the other hand, since the non-compensatory approach looks at single indicators independently, it classifies Dki Jakarta as exposed as Rangpur.

In Figure 5.4 one presents the global exposure map computed at the sub-national level with the non-compensatory DEA model. In short, results show that inhospitable regions, like tundras, deserts, and tropical forests are the least exposed areas to drought in the world. Since there is no or almost none human population, domestic animals, agriculture or industry in those regions,

Table 5.1: *Sub-national regions with the highest compensatory drought exposure values and respective: non-compensatory exposure values and normalized indicators' values.*

Region	Country	NC ¹	C ²	Pop ³	Agr ⁴	Ldens ⁵	IndDom ⁶
Rangpur	Bangladesh	1.000	0.487	0.074	1.000	0.870	0.002
Rajshahi	Bangladesh	0.965	0.466	0.079	0.944	0.840	0.002
Khulna	Bangladesh	0.775	0.371	0.063	0.770	0.649	0.001
Dhaka	Bangladesh	0.871	0.366	0.118	0.562	0.782	0.001
Kano	Nigeria	0.764	0.357	0.041	0.713	0.672	0.003
Ha Noi City	Vietnam	1.000	0.332	0.312	0.098	0.914	0.005
Katsina	Nigeria	0.822	0.320	0.022	0.497	0.760	0.001
West Bengal	India	0.777	0.319	0.081	0.481	0.706	0.006
Haryana	India	1.000	0.300	0.042	0.075	0.903	0.181
Delhi	India	0.958	0.297	0.740	0.084	0.253	0.110
Dki Jakarta	Indonesia	1.000	0.297	1.000	0.021	0.142	0.024
Ha Nam	Vietnam	1.000	0.285	0.071	0.064	1.000	0.004
Manouba	Tunisia	0.994	0.282	0.015	0.122	0.982	0.010
Hung Yen	Viet Nam	0.971	0.282	0.092	0.071	0.962	0.004
Punjab	Pakistan	0.806	0.282	0.037	0.265	0.623	0.202
Lwengo	Uganda	0.945	0.281	0.019	0.177	0.929	0.000
Barisal	Bangladesh	0.707	0.280	0.067	0.398	0.653	0.001
Quassim	Saudi Arabia	1.000	0.277	0.002	0.030	0.077	1.000

¹NC: Non-compensatory

²C: Compensatory

³Pop: Population density (people per sq. km of land area)

⁴Agr: Agricultural irrigated land (% of total agricultural land)

⁵Ldens: Livestock density (domestic animals per sq. km of land area)

⁶IndDom: Industrial and domestic water withdrawal as % of total renewable water resources (%)

this is an expected result and sustain the accuracy of the model for computing a map of global drought exposure.

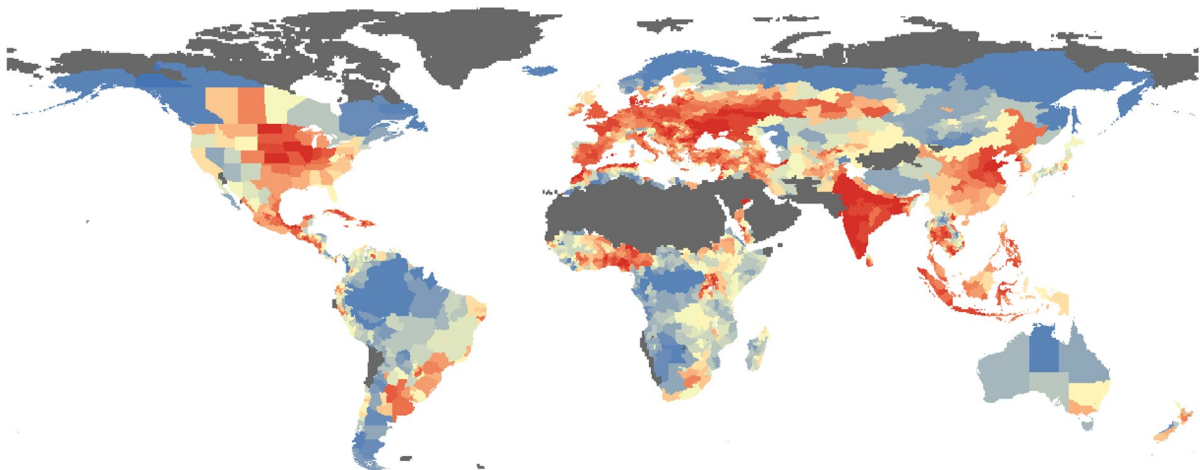


Figure 5.4: *Global map of drought exposure.*

Let us now look in more detail at the spatial distribution and intensity of exposure to drought in Latin America (Figure 5.5). On the one hand, and as similar as for the global context, the arid and semiarid regions of Latin America, such as South and West Argentina, North and South Chile, and North-West of Mexico are less exposed to drought. These areas have very

low population density and are barely used for agriculture, livestock or industrial activities. Therefore, direct or indirect human exposure to drought is none or almost nonexistent there. A similar situation occurs for the cross country sub-national regions covered by the Amazon humid ecosystem. The administrative regions comprised within this ecosystem are distinctly marked and categorized by an exposure to drought less than that of the remaining regions of the respective countries, which are not included in this ecosystem.

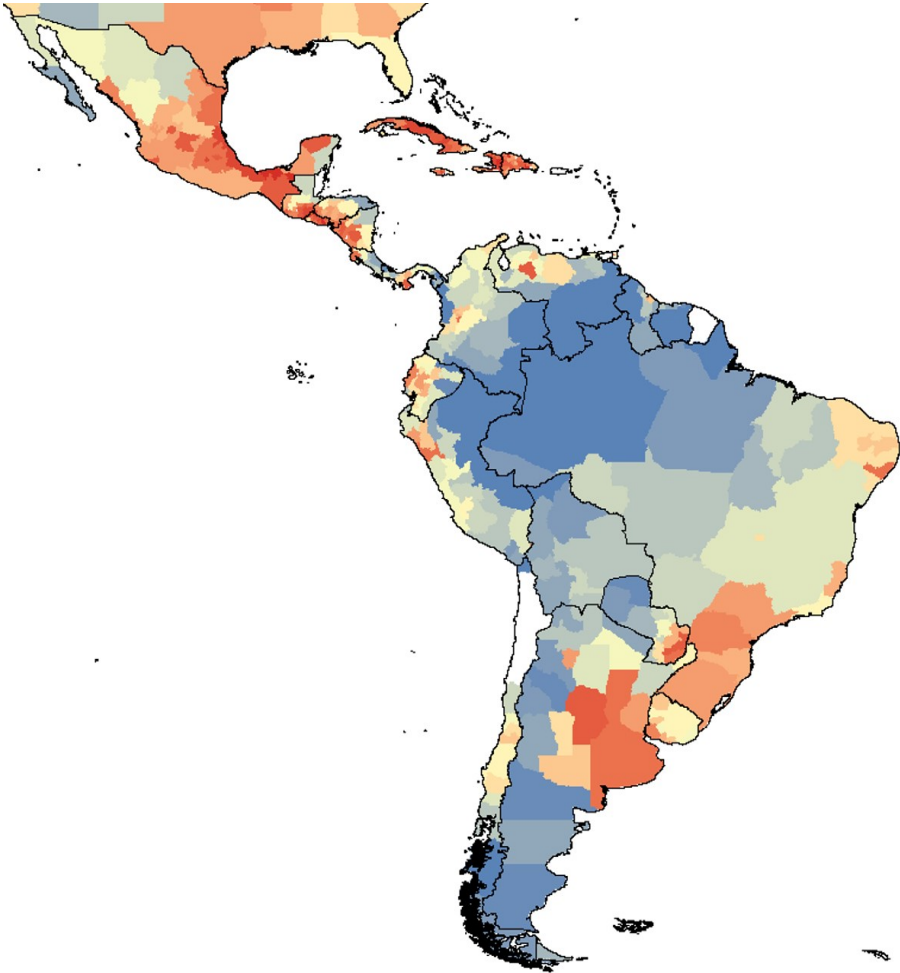


Figure 5.5: *Latin American map of drought exposure.*

Turning now to the exposed sub-national regions, we would like to highlight those of South to Southeast Brazil, North-West Argentina, Cuba, Southeast Mexico and some scattered areas in the west coast of South-America. According to [38], South and Southeast Brazil produce together more than 70% of the agriculture in the country, namely: the south is Brazil’s largest tobacco producer and the world’s largest exporter, whereas southeast produces almost 50% of the nation’s fruit and hosts 60% of agribusiness companies. In Argentina, the most exposed areas are the Chaco plain – fertile lowland in the northern region with subtropical rainforests and cotton farms; and the central Pampas – flat, fertile plains (a mix of humid and semi-arid areas) which provide much of Argentina’s agriculture including raising of sheep and cattle, and wheat, corn, soybean and fodder crops. In the case of the tropical rain forest of Southeast Mexico, fifty percent of it has been cut down and extensive natural pastures and field crops have been established in its place over the last 40 years [39]. Under these particular conditions and together with population increases of up to 207.1% for some municipalities [39], multispecies agroforestry cropping systems with cattle raising have developed and are a means by which the peasant families are able to maintain self-subsistence production. A remarkable feature of exposure to drought in Cuba is

the fact that 60% of its land is appropriate for agriculture, whereas the agricultural area in the other Latin American countries is about 34% of total land in average [40].

Interesting also to note that the geographical region of the Central American Dry Corridor (CADC) that extends over Guatemala, El Salvador, Honduras and Nicaragua is more exposed to drought than the sub-national regions of the respective countries not included in the CADC. Even that Central America is located in a tropical region with low hydric stress in a large part of its territory, drought risk is mentioned in many studies related to the CADC, as the impacts of droughts and floods usually threaten food security in the region. It is common to observe widespread impacts to these extreme events due to high exposure related to the dependency of populations on subsistence agriculture and livestock [41] [42] [43]. Indeed, from a total of 10.5 millions of people that live in the rural areas of the dry tropics (almost all in Nicaragua, Honduras, and Guatemala), close to 60% depend on subsistence agriculture and of deteriorated livelihoods [42]. On the other hand, for territories not covered by the CADC, e.g. Costa Rica, drought affects water supply for human consumption, agriculture, cattle rising and tourism [42] [43].

5.3 Drought Vulnerability

To evaluate and select the most suitable method for mapping global drought vulnerability, we computed and compared the mean distances between regional vulnerability ranks derived from the outputs of the models described in subsection 3.3 and the median regional vulnerability rank computed from the ensemble of all models, as described in subsection 4.4. We compare eight models that are tested for the aggregation of vulnerability factors derived from compensatory and non-compensatory conjunction of indicators by means of three approaches: arithmetic, geometric and the product.

In Figure 5.6, we vertically represent the distribution of vulnerability ranks computed for each administrative region by means of the tested models; regions are sorted horizontally in ascending order of the median rank computed from the ensemble of all models. Since the minimum and maximum ensemble values represent the limits of the interval in which regional vulnerability ranks fluctuate, then the most representative and robust measure of central tendency of the regional members of the ensemble, or general rank of regional vulnerability, is the median of the ensemble [34], as previously described in subsection 4.4.

Overall and with a single exception, the regional ranks derived from the non-compensatory conjunction of indicators within vulnerability factors are closer to the median of regional ranks computed from the ensemble of all models. The complete list of mean absolute distances to the median of regional ranks are presented in Table 5.2. The models showing shortest and largest mean ranking distances are, respectively *anCompVuln* and *aCompVuln*. These models are represented, respectively, by green and red dots in Figure 5.6.

Table 5.2: Mean distance of sub-national ranks to the median sub-national rank of the ensemble computed with different vulnerability models.

	anComp Vuln	gnComp Vuln	pnComp Vuln	aComp Vuln	gComp Vuln	pComp Vuln	wanComp Vuln	waComp Vuln
medR_i	81.67	83.88	96.59	181.23	146.59	96.15	119.57	93.12

To evaluate the reasons for the disparities in the distances between compensatory and non-compensatory models, let us look in detail at the outputs of *anCompVuln* and *aCompVuln* for six regions presented in Table 5.3. To ease the comparison, we make available the distribution of normalized physical vulnerability indicators for the presented regions. First, and as similar as for the exposure analysis performed in subsection 5.2, we immediately perceive that the asymptotic properties of the compensatory models lead to an unsatisfactory representation of vulnerability

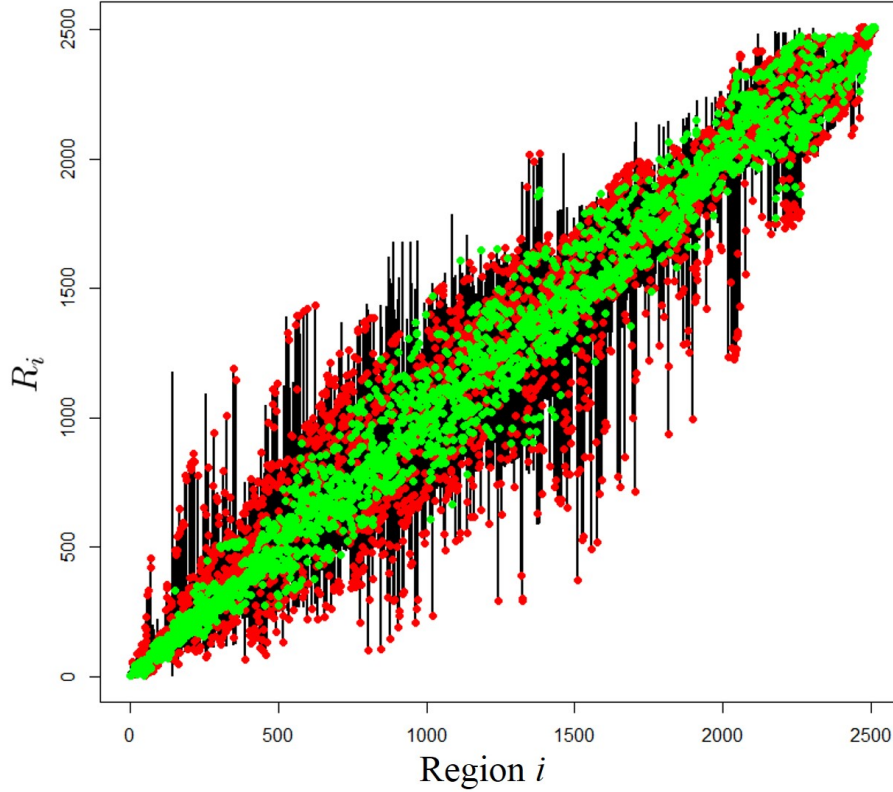


Figure 5.6: *Vulnerability to drought at sub-national regions ordered by the median ensemble rank: (black vertical lines) range of ensemble rank values; (red dots) rank of sub-national regions based on the model with maximum distance to median rank; (green dots) rank of sub-national regions based on the model with minimum distance to median rank.*

that is alleviated for the regional cases exhibiting extreme (contrasting) values for single (some of the) indicators within factors. For example, for regions that do not present important fluctuations of the normalized indicators, like Oestfold or Wanganui-m. (Table 5.3), both models perform alike. On the other hand, for regions that show a dispersed distribution of normalized physical indicators, like Zombo, Butha Buthe or Ngamiland, then the regional vulnerability to drought computed with the compensatory model is half of that computed with the non-compensatory approach. By smoothing regional discrepancies in the indicators' values, the compensatory model lessens vulnerability, causes regional values to converge asymptotically and the regional rankings to positioning distant from those attained with the non-compensatory model. For example, in a compensatory model it is assumed that the presence of irrigation infrastructures, e.g. like in the Ngamiland region, counterbalances a low water storage capacity for the region. From our viewpoint this is not the case and irrigation structures are useful only if water is able to be stored and available to be pumped for specific sectors of activity.

In Figure 5.7 we map the social (a), economic (b) and physical (c) factors computed with the non-compensatory approach and in Figure 5.8 we present the global vulnerability map computed with the model *anCompVuln*. Overall, results indicate that Central America, Northwest of South America, Africa – with the exception of South Africa, Central and South Asia are the most vulnerable regions to drought in the world. A detailed analysis of the factor maps presented in Figure 5.7, suggests that relatively high values of vulnerability to drought in Africa and Central America are function of simultaneously low physical, social and economic capacity. On the other hand, for South America and Central Asia, vulnerability is mainly due to a lack of physical capacity, whereas in South Asia there is a deficit of socio-economic capacity to manage the impacts of drought events.

Table 5.3: Indicators of physical factors for illustrative sub-national regions and respective vulnerability values computed models of average combination of non-compensatory (*anCompVuln*) and compensatory (*aCompVuln*) aggregation of indicators.

		Region (Country)					
		Zombo (Uganda)	Butha Buthe (Lesotho)	Ngamiland (Botswana)	O'Higgins (Chile)	Oestfold (Nor- way)	Wanganui- m. (New Zealand)
Model	<i>anCompVuln</i>	0.999	0.983	0.941	0.521	0.353	0.530
	<i>aCompVuln</i>	0.573	0.500	0.475	0.446	0.353	0.458
Factor	Indicators						
Phys.	Water	0.000	0.000	0.980	0.763	0.808	0.905
	Stor.						
	Road	0.612	0.224	0.817	0.807	0.721	0.918
	Dens.						
	Irrigated land	1.000	0.997	0.000	0.832	0.948	0.993

Regarding Latin America, the most striking result that emerges from the vulnerability analysis at the national level is the high intensity spot located at the middle latitude, namely covering the countries of Guatemala, El Salvador, Honduras and Nicaragua. Central America's population is growing rapidly, with average annual growth rates over the past ten years ranging from 1.6% in Panama to 2.6% in Honduras and Nicaragua [44]. Population growth increases exposure, as there are more people for a disaster to impact and because more assets (agriculture and livestock) settle in human managed areas (as previously discussed in subsection 5.2). In addition, population growth is related to poverty and this is a critical indicator underlying the economic vulnerability factor [45]. In these countries, an inverse relationship has been demonstrated between per capita GDP and total fertility rates, with countries having some of the highest fertility rates in the region among the poorest [44]. In addition, these countries show the highest percentage of rural population for Latin America. Rural societies may be more vulnerable to drought because of lower incomes and more dependence on a locally based resource economy (e.g. self-subsistence agriculture) [46].

On the other hand, it is also possible to identify intra-national differences of vulnerability to drought by sub-national administrative level, which are captured mainly by spatial discrepancies of physical indicators within a country. For example, North-West Brazil is more vulnerable to drought than the East and the South of the country; the fragmentation inside the nation is due to limited road network, water storage and irrigation structures in the regions covered by the Amazon forest.

5.4 Drought Risk

A final global drought risk map was computed at the first sub-national administrative level by means of Equation 2.1 and the products presented in Figs. 5.1, 5.4, and 5.8. The results on global drought risk are presented in Figure 5.9. At the first glance, one immediately perceives that regions with low or no exposure to drought (Fig. 5.4) show also low or no drought risk, namely tundras, deserts, and tropical forests. Tundras and tropical forests correspond also to the regions that are less affected by drought events (Fig. 5.1). Therefore, the remaining regions of the world are affected by more or less hazardous drought events and the risk depends on the degree of exposure and coping capacity (resilience in opposition to vulnerability, Fig. 5.8) to absorb or recover from the impacts of a drought. For example, the drought risk in U.S. is lower than Western Europe, and this last is lower than in South Asia.

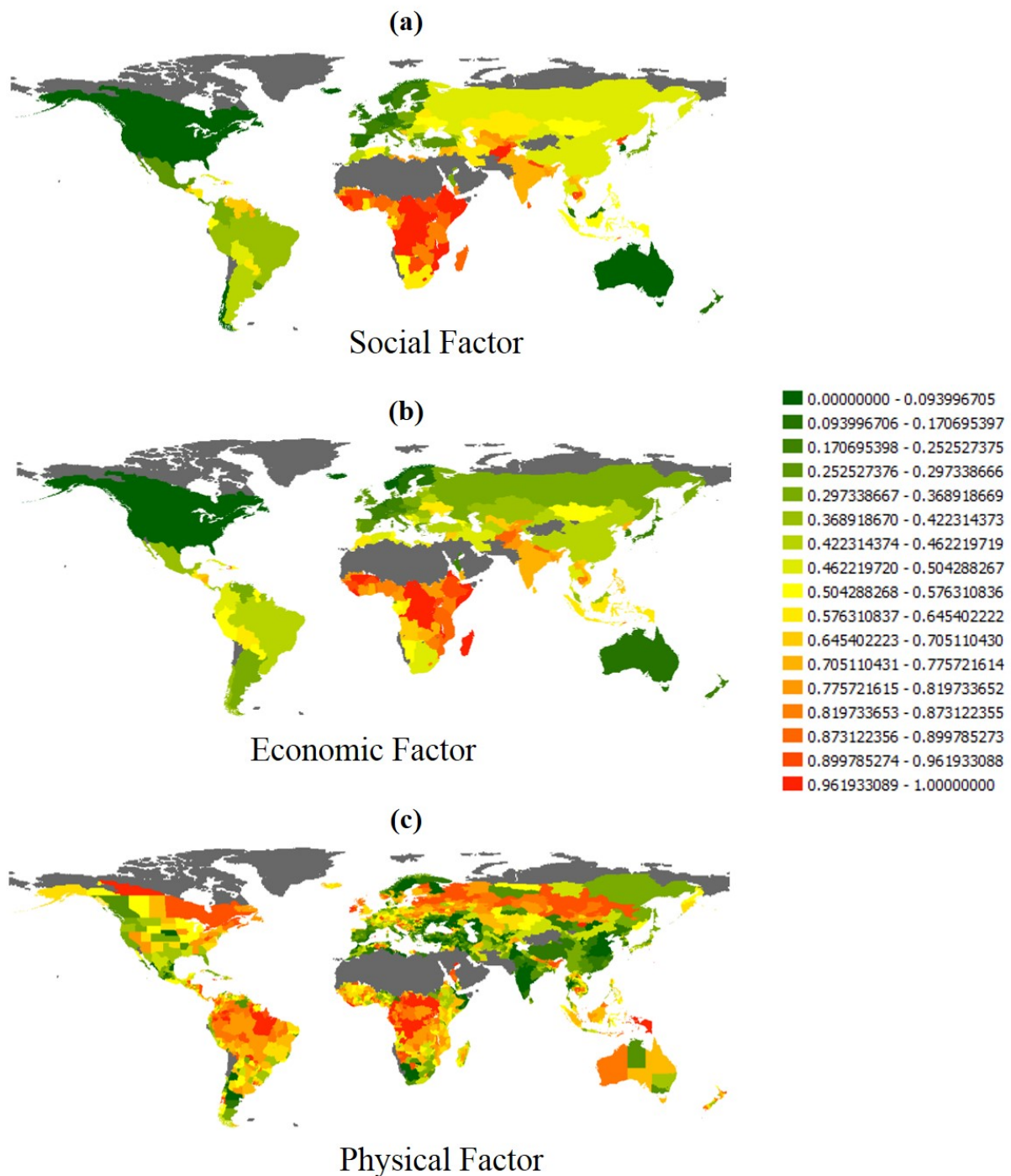


Figure 5.7: Global maps of drought vulnerability factors computed with the DEA approach.

To finish the discussion and focus in the problem of drought risk in Latin America, we would like to draw attention to two particular cross-country regions: the CADC and the Southeast Brazil/Northeast Argentina. The common determinant of risk in these regions is drought exposure: it is similarly high because both regions are densely populated (rural communities in CADC in contrast to urban communities in Brazil/Argentina) and resemble by having large areas allocated for agricultural production (self-subsistence in CADC in contrast to cash crops in Brazil/Argentina). The distinctive determinants are the higher vulnerability in CADC and the higher hazard in Brazil/Argentina. Even though Brazil/Argentina have more economic, social and infrastructural resources to mitigate and delay the effects of a drought, the drought risk in

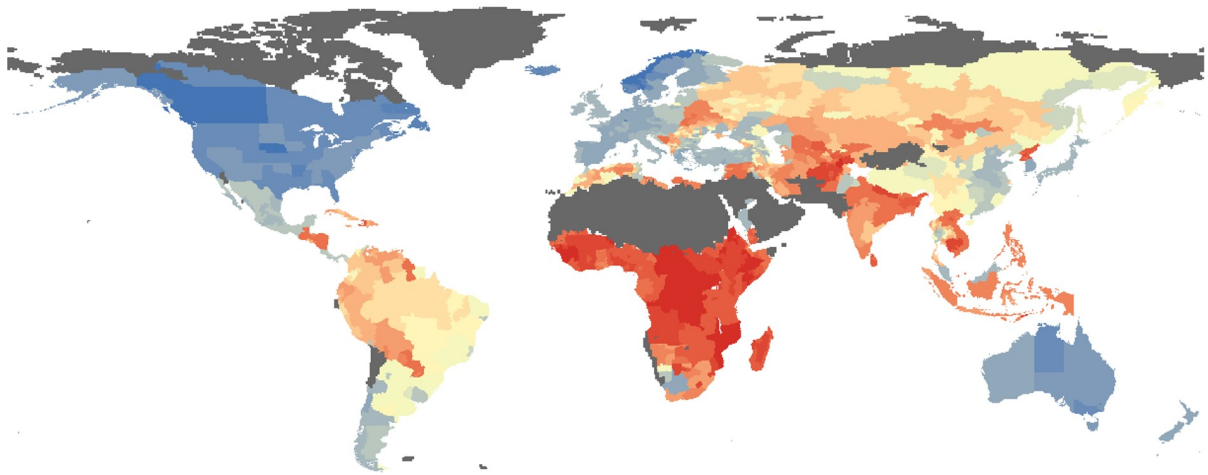


Figure 5.8: *Global map of drought vulnerability.*

the east coast is high because severe and prolonged droughts often strike there. Drought events that spread over several years will have serious economic and social impacts from the local to national scales as those regions are the centers of primary sectors of activity of the respective countries. On the other hand, drought risk in the Central America is high because the subsistence of typical rural communities depend on yearly crop yields. Therefore, rare and short drought events of mild intensity that strike during growing period of rainfed crops can have serious impacts on local populations that do not have the economic, social and physical abilities to cope with it. The results of this study show that although different in structure and composition, both regions require great attention from stakeholders, policymakers, scientific networks and the respective communities, for defining adequate mitigation and adaptation measures, while increasing sustainability and bring down the impacts of future drought events.

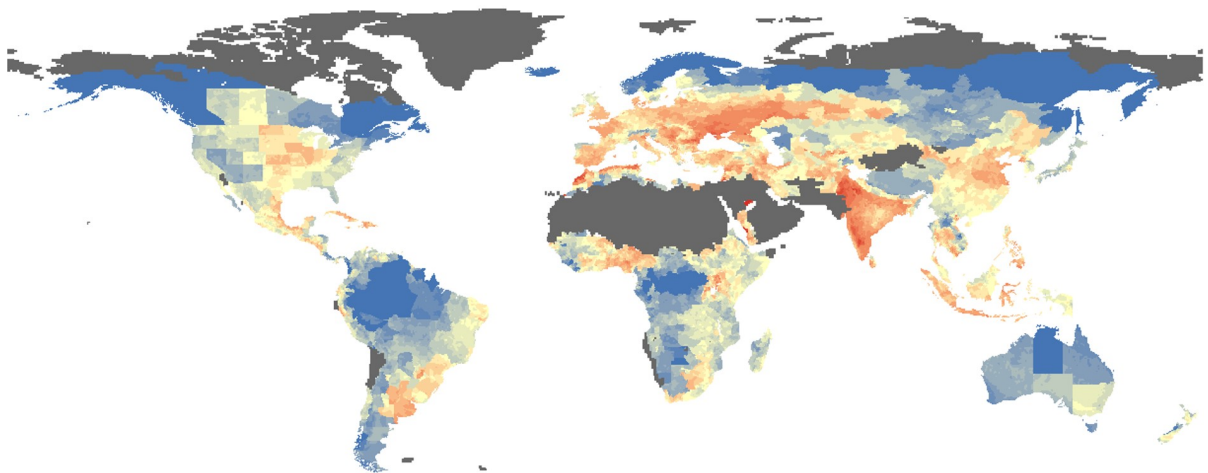


Figure 5.9: *Global map of drought risk.*

6 Conclusions

This technical report presents the formulation, validation and selection of a global drought risk model that is derived from the combination of global drought hazard, exposure and vulnerability determinants. An extended analysis of the attained results focus on Latin America, as this study is part of the activities developed in the framework of Component 3 of the second phase of the Programme EUROCLIMA: “Sustainable Agriculture, Food Security and Climate Change in Latin America: Strengthening the capacities of key stakeholders to adapt agriculture to climate change and mitigate its effects”. We decided to conduct our analysis from a global to a continental perspective (in order to place Latin America in the globe), and finally to look at the national and sub-national scales of risk and its determinants in Latin America, as the models we propose are of relative/standardized intensity. Since the approach is relative and Latin America is part of a global community that interact, share and support each other social, economic and physically, each country (or sub-national administrative region, or local area) is compared with each other and ranked according to some predefined or empirically determined benchmark derived from the environmental, physical, economic and social characteristics of the analyzed regions.

We propose a data driven approach for computing each determinant of risk and derive a final global map based on the theoretical formulation proposed by the UNSDRI [1]. Drought risk is computed at the sub-national administrative level to facilitate the management of global layers and their association on a fix and common Minimum Mapping Unit (MMU). Moreover, products delivered at the level of administrative regions are also useful and easy to manipulate by stakeholders and policy makers. Each determinant of risk is formulated independently of each other and validated on its own. The results presented in this report are promising and in general match the expected patterns of global drought determinants and risk. To the best of our knowledge, this is the first attempt to systematically map drought risk and its components at the global level by means of a consistent and standardized approach and using high spatial resolution input datasets of analysis that meet the interests of stakeholders and policymakers.

Nevertheless, there are several points that can be used for discussion and improvement of the final products. Regarding drought hazard, the main difficulties relate with the definition of thresholds to identify drought onset and end, as well as the magnitude of droughts for which events are considered hazardous. In this report, we describe a methodological approach that focus on an optimized classification algorithm to determine the onset and end of a drought. This can be fine tuned by using other approaches or by expert knowledge. In addition, the methodological approach proposes the use of the median global standardized drought severity as a reference to identify hazardous drought events. Although the presented results show a good match with the global occurrence of historical drought events reported in the literature, we are of the opinion that this threshold can also be fine tuned nationally or identified locally by expert knowledge to improve the accuracy of the method at an higher spatial resolution.

Drought exposure is computed by combining thematic geographic layers of population and livestock density, agriculture intensity and water pressure for industrial and domestic use. These layers have different input spatial resolution, encoding formats and were uniformly generalized at the sub-national administrative level. We report four types of production errors and/or limitations in the geographic datasets that can lessen the quality of the final exposure layer: thematic accuracy, geographic positioning, reference date of input datasets, and the generalization process to a common MMU. Moreover, as the final exposure map is a combination of these generalized layers, a propagation of errors can also reduce the accuracy of the final results. This propagation process is more critical because we have based our analyses on global datasets that might have a different accuracy for different geographic regions. A neater solution would be to use an hybrid product derived by merging local to regional datasets of improved thematic and geographic accuracy. For example, for Europe, the distribution of agriculture could be improved with the use of the CORINE Land Cover (CLC) [47], and in Brazil with the use of the national Land Use map [48]. However, the processing of local products raises the problem of thematic

harmonization: for example, the harmonization of the CLC classification system with that of the Brazilian land use map and other regional products for, e.g. the United States or Australia, is not straightforward and might introduce larger errors in the global equilibrium of relative exposure. So far, a limitation of the proposed approach is the fact that only human managed regions are analyzed, i.e. no environmental layers of protected areas, degraded ecosystems and others are considered in the model.

Regarding vulnerability, a major limitation of the proposed approach is the use of national information for computing the model – it might be criticized by the lack of spatial detail. This solution is the best compromise for the time being, since harmonized databases with socio-economic information at sub-national administrative level were not freely retrieved at the global level. Nevertheless, it is important to highlight that in the case this information would be available, other difficulties on their harmonization would arise. For example, the intra-national management of regional disparities is not easily understood when a hazard strikes: some countries might set out immediate national support to their poorer regions and others do not have this capacity. The richest region in some poor country might not respond to a hazard alike the poorest region in some rich country. Therefore, we are of the opinion that the use of socio-economic factors at the national level is a limitation in this study, but it is simultaneously a good compromise between unknown multi-scale relationships (that would increase the bias in the model and lower thematic accuracy) and output knowledge of high spatial resolution. A second limitation relates with the selection of the model. We based our decision on an internal validation procedure that votes the best model as the one giving regional vulnerability ranks that approximate the median of the ensemble of all models tested. A neater solution could be tested, but the absence of reference data for performing an independent validation reduces the lack of valid testing options.

Regarding drought risk in Latin America, attained results show that hazard is higher in Southeast and Northeast Brazil, between the Northeast and Southwest of Argentina, as well as the whole Southern part of the country; exposure is higher in Southeast Brazil and Northeast Argentina, as well as in the Central American Dry Corridor (CADC); vulnerability is higher in CADC region. Overall, and due to regional differences in the characteristics of its determinants, drought risk is more prominent in Central America and Southeast of South America. Since the determinants of risk vary in these areas, we are of the opinion that there are no single management approximations to drought mitigation and adaptation measures should be evaluated independently and fit to the demands of each case.

References

- [1] UNSDIR, Living with risk: A global review of disaster reduction initiatives, Review Volume 1, United Nations International Strategy for Disaster Reduction, New York and Geneva (2004).
- [2] J. Spinoni, J. Vogt, G. Naumann, H. Carrao, P. Barbosa, Towards identifying areas at climatological risk of desertification using the kppengeiger classification and fao aridity index, *International Journal of Climatology* 35 (9) (2015) 2210–2222.
- [3] A. K. Mishra, A. K., V. P. Singh, A review of drought concepts, *J. Hydrol.* 391 (2009) 202–216.
- [4] D. A. Wilhite, M. H. Glantz, Understanding the drought phenomenon: The role of definitions, *Water Int.* 10 (1985) 111–120.
- [5] R. R. Heim, A review of twentieth-century drought indices used in the united states, *Bull. Am. Meteorol. Soc.* 83 (2002) 1149–1165.
- [6] J. Keyantash, J. A. Dracup, The quantification of drought: An evaluation of drought indices, *Bull. Am. Meteorol. Soc.* 83 (2002) 1167–1180.
- [7] H. Carrão, A. Singleton, G. Naumann, P. Barbosa, J. Vogt, An optimized system for the classification of meteorological drought intensity with applications in frequency analysis, *J. Appl. Meteor. Climatol.* 53 (2014) 1943–1960.
- [8] G. Magrin, C. G. Garca, D. C. Choque, J. C. Gimnez, A. R. Moreno, G. J. Nagy, C. Nobre, , A. Villamizar, Climate change 2007: Impacts, adaptation and vulnerability, in: M. L. Parry, O. F. Canziani, J. P. Palutikof, P. J. van der Linden, C. E. Hanson (Eds.), *Contribution of Working Group II to the Fourth Assessment Report of the Intergovernmental Panel on Climate Change*, Cambridge University Press, 2007, pp. 581–615.
- [9] WWF, Rich Countries, Poor Water, [Available online at <http://www.wwf.org.uk/filelibrary/pdf/richcountriespoorwater.pdf>] (cited 6 August 2015).
- [10] A. Lavell, M. Oppenheimer, C. Diop, J. Hess, J. L. R. Lempert, R. Muir-Wood, S. Myeong, Climate change: new dimensions in disaster risk, exposure, vulnerability, and resilience, in: C. Field, V. Barros, T. Stocker, D. Qin, D. Dokken, K. Ebi, M. Mastrandrea, K. Mach, G.-K. Plattner, S. Allen, M. Tignor, P. Midgley (Eds.), *Managing the Risks of Extreme Events and Disasters to Advance Climate Change Adaptation – Report of Working Groups I and II of the Intergovernmental Panel on Climate Change (IPCC)*, Cambridge University Press, Cambridge, UK, and New York, NY, USA, 2012, pp. 25–64.
- [11] P. Peduzzi, H. Dao, C. Herold, F. Mouton, Assessing global exposure and vulnerability towards natural hazards: the disaster risk index, *Natural Hazards and Earth System Science* 9 (4) (2009) 1149–1159.
- [12] H. Dao, P. Peduzzi, Global risk and vulnerability index trends per year (gravity), Technical annex and multiple risk integration Phase IV, UNDP/BCPR, Geneva (2003).
- [13] UNDRO, Natural disasters and vulnerability analysis, Report of the expert group meeting (9–12july 1979), Office of the United Nations Disaster Relief Co-ordinator, Geneva (1980).
- [14] H. Carrão, P. Barbosa, J. Vogt, Assessing and mapping drought hazard in africa and south-central america with a meteorological drought severity index, in: *Geophysical Research Abstracts*, Vol. 17, EGU2015, European Geosciences Union (EGU), Vienna, Austria, 2015, p. 15453.

- [15] S. Shahid, H. Behrawan, Drought risk assessment in the western part of bangladesh, *Natural Hazards* 46 (3) (2008) 391–413.
- [16] T. Downing, K. Bakker, Drought discourse and vulnerability, in: W. D.A. (Ed.), *Drought: A Global Assessment*, Natural Hazards and Disasters Series, Routledge Publishers: UK, 2000, pp. 213–230.
- [17] G. Naumann, P. Barbosa, L. Garrote, A. Iglesias, J. Vogt, Exploring drought vulnerability in africa: an indicator based analysis to be used in early warning systems, *Hydrology and Earth System Sciences* 18 (5) (2014) 1591–1604.
- [18] P. Blaikie, T. Cannon, I. Davis, B. Wisner, *At Risk: Natural Hazards, People’s Vulnerability and Disasters*, At Risk: Natural Hazards, People’s Vulnerability, and Disasters, Taylor & Francis, 1994.
- [19] I. Burton, R. Kates, G. White, *The Environment as Hazard*, 2nd Edition, Guilford Press, 1993.
- [20] A. Becker, P. Finger, A. Meyer-Christoffer, B. Rudolf, K. Schamm, U. Schneider, M. Ziese, A description of the global land-surface precipitation data products of the global precipitation climatology centre with sample applications including centennial (trend) analysis from 1901present, *Earth System Science Data* 5 (1) (2013) 71–99.
- [21] C.-L. Hwang, K. Yoon, *Multiple Attribute Decision Making: Methods and Applications, A State-of-the-Art Survey*, Lecture Notes in Economics and Mathematical Systems, Springer Berlin Heidelberg, 1981.
- [22] C. Lovell, J. T. Pastor, Radial {DEA} models without inputs or without outputs, *European Journal of Operational Research* 118 (1) (1999) 46 – 51.
- [23] W. D. Cook, K. Tone, J. Zhu, Data envelopment analysis: Prior to choosing a model, *Omega* 44 (2014) 1–4.
- [24] OECD/JRC, *Handbook on constructing composite indicators. Methodology and user guide*, Social Policies and Data Series, OECD Publisher, Paris, 2008.
- [25] N. Brooks, W. N. Adger, P. M. Kelly, The determinants of vulnerability and adaptive capacity at the national level and the implications for adaptation, *Global Environmental Change* 15 (2) (2005) 151 – 163.
- [26] I. Scoones, *Sustainable rural livelihoods: A framework for analysis*, Working Paper 72, Institute of Development Studies (IDS), Brighton (1998).
- [27] UNDP, *The rise of the south: Human progress in a diverse world*, Human Development Reports 19902013 23, United Nations Development Programme, New York, USA (2013).
- [28] S. Alkire, M. Santos, Measuring acute poverty in the developing world: Robustness and scope of the multidimensional poverty index, *World Development* 59 (2014) 251–274.
- [29] UNEP, *World atlas of desertification*, Middleton, n.j. and thomas, d.s.g.(eds.), United Nations Environment Programme, London; Baltimore: Edward Arnold Sevenoaks (1992).
- [30] T. Mitchell, P. Jones, An improved method of constructing a database of monthly climate observations and associated highresolution grids, *International Journal of Climatology* 25 (2005) 693–712.

- [31] M. Ziese, U. Schneider, A. Meyer-Christoffer, P. Finger, K. Schamm, A. Becker, B. Rudolf, A combined drought index from the global precipitation climatology centre (gpcc), in: Geophysical Research Abstracts, Vol. 15, EGU2013, European Geosciences Union (EGU), Vienna, Austria, 2013, p. 4158.
- [32] T. Hayden, National Geographic Atlas of the world, Ninth Edition, National Geographic Society, 2008.
- [33] E. W. Steyerberg, S. E. Bleeker, H. A. Moll, D. E. Grobbee, K. G. Moons, Internal and external validation of predictive models: A simulation study of bias and precision in small samples, *Journal of Clinical Epidemiology* 56 (5) (2003) 441 – 447.
- [34] D. S. Wilks, *Statistical Methods in the Atmospheric Sciences*, 2nd Edition, Academic Press, 2005.
- [35] Brasil-MMA, National action program to combat desertification and mitigate the effects of drought: Pan-brazil, MMA Editions ISBN 85-87166-66-2, Environment Ministry, Water Resources Secretariat, Brasília, Brasil (2004).
- [36] Brasil-MI/MMA/MCT, Relatório final do grupo de trabalho interministerial para redefinição do semiárido nordestino e do polígono das secas, Tech. rep., Presidência da República, Brasília, Brasil (2005).
- [37] S. Russo, A. Dosio, A. Sterl, P. Barbosa, J. Vogt, Projection of occurrence of extreme dry-wet years and seasons in europe with stationary and nonstationary standardized precipitation indices, *Journal of Geophysical Research: Atmospheres* 118 (14).
- [38] J. L. Parré, J. J. M. Guilhoto, A desconcentração regional do agronegocio brasileiro, *Revista Brasileira de Economia* 55 (2001) 223–251.
- [39] M. Alvarez-Buylla Roces, E. Lazos Chavero, J. Garca-Barrios, Homegardens of a humid tropical region in southeast mexico: an example of an agroforestry cropping system in a recently established community, *Agroforestry Systems* 8 (2) (1989) 133–156.
- [40] FAO, Aquastat database - food and agriculture organization of the united nations (fao), [Available online at <http://www.fao.org/nr/water/aquastat/main/index.stm>.] (cited 18/11/2014).
- [41] O. P. Rodríguez, J. C. Alocn, C. Z. Elvir, Buenas prácticas para la seguridad alimentaria y la gestión de riesgo, *Acción contra el Hambre (ACF) 19627*, Organización de las Naciones Unidas para la Alimentación y la Agricultura (FAO), Tegucigalpa, Honduras (2012).
- [42] A. van der Zee Arias, J. van der Zee, A. Meyrat, C. Poveda, L. Picado, Estudio de la caracterización del corredor seco centroamericano, *Acción contra el Hambre (ACF) Pases CA-4*, Organización de las Naciones Unidas para la Alimentación y la Agricultura (FAO), Tegucigalpa, Honduras (2012).
- [43] A. van der Zee Arias, J. van der Zee, A. Meyrat, C. Poveda, L. Picado, Identificación de actores relevantes y relaciones interinstitucionales en el corredor seco centroamericano, *Acción contra el Hambre (ACF) Pases CA-4*, Organización de las Naciones Unidas para la Alimentación y la Agricultura (FAO), Tegucigalpa, Honduras (2012).
- [44] R. Pielke, J. Rubiera, C. Landsea, M. Fernandez, R. Klein, Hurricane vulnerability in latin america and the caribbean: Normalized damage and loss potentials, *Natural Hazards Review* 4 (3) (2003) 101–114.

- [45] A. Lavell, Prevention and mitigation of disasters in central america: Vulnerability to disasters at the local level, in: A. Varley (Ed.), Disasters, development, and environment, Wiley, New York, 1994, pp. 49–63.
- [46] S. L. Cutter, B. J. Boruff, W. L. Shirley, Social vulnerability to environmental hazards*, Social Science Quarterly 84 (2) (2003) 242–261.
- [47] G. Büttner, B. Kosztra, G. Maucha, R. Pataki, Implementation and achievements of clc2006, Tech. rep., European Environment Agency (EEA) (2010).
- [48] IBGE, Manual técnico de uso da terra, Manuais técnicos em geociências 7, Instituto Brasileiro de Geografia e Estatística, Rio de Janeiro, Brasil (2013).



JRC Mission

As the Commission's in-house science service, the Joint Research Centre's mission is to provide EU policies with independent, evidence-based scientific and technical support throughout the whole policy cycle.

Working in close cooperation with policy Directorates-General, the JRC addresses key societal challenges while stimulating innovation through developing new methods, tools and standards, and sharing its know-how with the Member States, the scientific community and international partners.

*Serving society
Stimulating innovation
Supporting legislation*

